JAEA-Review
2017-014
DOI:10.11484/jaea-review-2017-014

JAEA-Review

Geopolymers and Their Potential Applications in the Nuclear Waste Management Field - A Bibliographical Study -

Vincent CANTAREL, Takafumi MOTOOKA and Isao YAMAGISHI

Waste Management Division
Collaborative Laboratories for Advanced Decommissioning Science
Sector of Fukushima Research and Development

June 2017

Japan Atomic Energy Agency

日本原子力研究開発機構

本レポートは国立研究開発法人日本原子力研究開発機構が不定期に発行する成果報告書です。
本レポートの入手並びに著作権利用に関するお問い合わせは、下記あてにお問い合わせ下さい。
なお、本レポートの全文は日本原子力研究開発機構ホームページ（http://www.jaea.go.jp）
より発信されています。

国立研究開発法人日本原子力研究開発機構 研究連携成果展開部 研究成果管理課
〒319-1195 茨城県那珂郡東海村大字白方 2 番地4
電話 029-282-6387, Fax 029-282-5920, E-mail:ird-support@jaea.go.jp

This report is issued irregularly by Japan Atomic Energy Agency.
Inquiries about availability and/or copyright of this report should be addressed to
Institutional Repository Section,
Intellectual Resources Management and R&D Collaboration Department,
Japan Atomic Energy Agency.
2-4 Shirakata, Tokai-mura, Naka-gun, Ibaraki-ken 319-1195 Japan
Tel +81-29-282-6387, Fax +81-29-282-5920, E-mail:ird-support@jaea.go.jp

JAEA-Review 2017-014

Geopolymers and Their Potential Applications in the Nuclear Waste Management Field
-A Bibliographical Study -

Vincent CANTAREL※, Takafumi MOTOOKA and Isao YAMAGISHI

Waste Management Division
Collaborative Laboratories for Advanced Decommissioning Science
Sector of Fukushima Research and Development
Japan Atomic Energy Agency
Tokai-mura, Naka-gun, Ibaraki-ken

(Received April 28, 2017)

After a necessary decay time, the zeolites used for the water decontamination will eventually be conditioned for their long-term storage. Geopolymer is considered as a potential matrix to manage radioactive cesium and strontium containing waste. For such applications, a correct comprehension of the binder structure, its macroscopic properties, its interactions with the waste and the physico-chemical phenomena occurring in the wasteform is needed to be able to judge of the soundness and viability of the material.

Although the geopolymer is a young binder, a lot of research has been carried out over the last fifty years and our understanding of this matrix and its potential applications is progressing fast. This review aims at gathering the actual knowledge on geopolymer studies about geopolymer composites, geopolymer as a confinement matrix for nuclear wastes and geopolymer under irradiation. This information will finally provide guidance for the future studies and experiments.

Keywords: Geopolymer, Nuclear Waste, Irradiation, Wasteform, Metakaolin

---

※Post-Doctoral Fellow

ジオポリマーとその核廃棄物管理分野での適用可能性について
ー文献調査ー

日本原子力研究開発機構
福島研究開発部門
廃炉国際共同研究センター
廃棄物処理処分ディビジョン

Vincent Cantarel※、本岡　隆文、山岸　功

（2017 年 4 月 28 日 受理）

十分な崩壊時間の後、水の除染に使用されたゼオライトは、最終的に長期保管のために処理される。ジオポリマーは、放射性セシウムおよびストロンチウム含有廃棄物の管理にあたり有望な固定基材と考えられている。 このような用途のためには、バインダー構造、その巨視的性質、廃棄物との相互作用、および廃棄物形態で生じる物理化学的現象の正確な理解が、材料の健全性および安定性を判断する上で必要である。

ジオポリマーは歴史の浅いバインダーであるが、この50年間に多くの研究が行われており、その特性とその用途の理解は急速に進んでいる。本レビューでは、ジオポリマーに関する研究から、ジオポリマー複合材料、核廃棄物固化材料、照射下のジオポリマーについて、実用的な情報を収集している。取集した情報は、今後の研究と実験のためのガイダンスとして活用する。

原子力科学研究所：319-1195　茨城県那珂郡東海村大字白方 2 番地 4
※博士研究員

Contents

1. Introduction 1

2. Geopolymers 2
2.1 Synthesis – geopolymerization 2
2.2 Structure and properties of geopolymers 2
2.2.1 Structure 3
2.2.2 Porosity 3
2.2.3 Mechanical strength 3
2.2.4 Alkali silica reaction 3
2.2.5 Carbonation 4
2.2.6 Acid resistance 4
2.2.7 Thermal resistance 4
2.2.8 Temporal evolution and durability 5
2.3 Formulation 5
2.3.1 Alkali cation 5
2.3.2 M/Al ratio (M = Na, K or Cs) 6
2.3.3 Si/Al ratio 7
2.3.4 Water content 7
2.3.5 Raw materials 8
2.4 Unascertained or unexplored 8

3. Geopolymer composites 9
3.1 Sand and aggregates 9
3.2 Inorganic fibers (non metallic) 9
3.3 Organic fibers 10
3.4 Metal 10

4. Geopolymer solidification of nuclear wastes 11
4.1 Sludge, resin, liquid wastes and their mixtures 11
4.2 Zeolites 11
4.3 Magnox swarf – Aluminum metal 13
4.4 Mg-Zr alloys from UNGG reactors 13
4.5 Graphite 14
4.6 Salts 14
4.7 Cobalt ($CoCl_2$) 15
4.8 Organic liquids 16
4.9 Contaminated water 16
4.10 Secondary waste in Fukushima Daiichi NPS 16
4.11 Miscellaneous 17

5. Geopolymer under irradiation 19
5.1 Behavior under gamma irradiation 19
5.2 Behavior under electron irradiation 21
5.2.1 Structural modifications 21
5.2.2 Creation of radicals 21

5.3 Behavior under heavy ion irradiation 22
5.3.1 Chemical structure evolution 22
5.3.2 Porosity evolution 23
5.3.3 Dihydrogen production 23
5.4 Behavior as neutrons absorber 23

6. Conclusions 25

References 26

目 次

1. 緒言 1

2. ジオポリマー 2
2.1 ジオポリマーの重合化 2
2.2 ジオポリマーの構造と性質 2
2.2.1 構造 3
2.2.2 気孔 3
2.2.3 機械的強度 3
2.2.4 アルカリシリカ反応 3
2.2.5 炭酸化 4
2.2.6 耐酸性 4
2.2.7 耐熱性 4
2.2.8 時間劣化と耐久性 5
2.3 調製 5
2.3.1 アルカリカチオン 5
2.3.2 M/Al 比率 (M = Na, K or Cs) 6
2.3.3 Si/Al 比率 7
2.3.4 含水量 7
2.3.5 原材料 8
2.4 不明点 8

3. ジオポリマー複合 9
3.1 砂と骨材 9
3.2 無機繊維(非金属) 9
3.3 有機繊維 10
3.4 金属 10

4. 原子力産業におけるジオポリマー 11
4.1 スラッジ、樹脂、液体廃棄物とそれらの混合物 11
4.2 ゼオライト 11
4.3 マグノックスの切屑 – 金属アルミニウム 13
4.4 UNGG 原子炉からの Mg-Zr 合金 13
4.5 黒鉛 14
4.6 塩類 14
4.7 コバルト ($CoCl_2$) 15
4.8 有機液体 16
4.9 汚染水 16
4.10 福島第一原発の二次廃棄物 16
4.11 未定義の廃棄物 17

5. 照射下のジオポリマー 19
5.1 ガンマ線照射下での挙動 19
5.2 電子線照射下での挙動 21
5.2.1 構造変化 21
5.2.2 ラジカル生成 21
5.3 重イオン照射下での挙動 22
5.3.1 化学構造変化 22
5.3.2 空隙発生 23
5.3.3 水素発生 23
5.4 中性子吸収剤としての挙動 23

6. まとめ 25

参考文献 26

Figures List

Figure 1 Schematic representation of Provis reaction model [2] between an activating alkaline solution and an aluminosilicate source with a low calcium content 32
Figure 2 Representation of the structure of a sodium based geopolymer..... 32
Figure 3 Representation of the relations between macroscopic properties and formulation parameters 33
Figure 4 Schematic representation by F. Chupin [23] (translated) of water radiolysis in geopolymer under gamma or heavy ion irradiation..... 34

Tables List

Table 1 Specific surface, mean pore diameter and pore volume obtained by P. Steins [48] with geopolymer having the same formulation: 1.8 Si/M ; 1 Al/M ; 11.5 H_2O/M with M = Na, K or Cs..... 35
Table 2 Studies and patents about geopolymer as a matrix for nuclear wastes ordered by country 35
Table 3 Cs leaching results of Deng et al. [126] 36

This is a blank page.

1. Introduction

Geopolymers are inorganic binders. This name was given during the 70's by Davidovitz with reference to inorganic or mineral materials [1]. Geopolymers have a network structure formed by aluminates and silicates tetrahedrons. They are included in the material class of activated materials and their hardening mechanism, called geopolymerization, is essentially based on the poly-condensation of aluminosilicates tetrahedrons [2,3]. The aluminum present in the structure comes from an aluminosilicate reactant in alkaline media such as metakaolin or fly ashes. The silica comes from both of this aluminosilicate source and dissolved silica. An aqueous solution, containing silica and hydroxides is thus used to activate the metakaolin. This solution is usually called "activating solution". It can be made either by dissolution of silica in an alkali hydroxide solution or by composition adjustment of a waterglass solution by addition of an alkali hydroxide and water. To be able to compare different formulations, a geopolymer is often defined using the ceramist nomenclature, giving the molar ratio of the different oxides present in final the matrix. For example, 1 Al_2O_3; 4 SiO_2; 1 Na_2O; 11 H_2O.

In the literatures, the word "geopolymers" can also sometime refer to other alkali-activated binders with consequent calcium contents. Even if the final materials are macroscopically similar, their structure differs by the presence, for example, of CSH (calcium silicate hydrate) or CASH phases (calcium aluminum silicate hydrate) and the transferability of scientific results is subject to discussion. This bibliographic study will only focus on geopolymers based on metakaolin or fly ashes with a low calcium content (Class F fly ashes). Thus, in this review, studies using activated slags, Class C fly ash or other activate materials containing a consequent fraction of calcium are not mentioned.

This document is structured in four parts. The first part is focused on geopolymers pastes (pure geopolymers). Their synthesis, structure and main properties are described. Then, the actual knowledge on the influence of each formulation parameter is briefly outlined. The second part aims at giving a quick overview of the literatures experiments concerning the incorporation of some classical filler / reinforcement in a geopolymer. The incorporation of nuclear waste is intentionally eluded as the next part will be dedicated to an exhaustive review the applications of geopolymers in the nuclear waste management field. At last, the results of the literature concerning the behavior of geopolymer under irradiation are presented.

This bibliographic study was mainly effected using the database of web of science. For the first part, four recent Ph.D. theses were also extensively referred. For information about the usage of geopolymers for nuclear waste management, AIEA documents, google patent and espacenet were also consulted.

2. Geopolymers

2.1 Synthesis – geopolymerization

The geopolymerization is the reaction, at ambient temperature, between a concentrated alkali silicate solution and an aluminosilicate source. In specific conditions, a monolithic amorphous network is formed and called geopolymer.

Reactions and kinetics of geopolymerization are complex, and studies are still being carried out to understand them completely [4–6]. In 1985, Babushkin [7] proposed reactions based on the dissolution of the aluminosilicate source followed by a poly-condensation of aluminosilicate species. These reactions allowed to define a first geopolymerization mechanism, developed in other publications [6,8–11] (Figure 1).

The most currently admitted phenomenology is the following. The hydrolysis/dissolution step occurs when the aluminosilicate source is added to an alkaline solution. As a result, silicates and aluminates monomers are formed by the Si-O-Si and Si-O-Al bond breaking [12]. These entities do not possess any bonds with another silicate or aluminum atom. These monomers react together to form small oligomers up to an equilibrium state. This is the restructuration step. This step is determining for the formation of the geopolymer microstructure and the pore size distribution [13,14]. At last, when the solution becomes oversaturated in oligomers, they, in turn, can poly-condense to a first polymeric gel. This is the poly-condensation step. After the formation of this first gel, the system continues to reorganize. Previously described entities polymerize to form a tridimensional network increasingly connected.

With the polymerization, the system loses mobility: it hardens and a percolating network is obtained. Indeed, following the evolution of rheological moduli of a geopolymer paste, two step can be identified [15]: A first step with low modification of the rheological moduli corresponding to the concomitant reactions of dissolution and formation of the first oligomers and aggregates, followed by a sharp increase of the moduli induced by the formation of a percolating network. After the percolation, the geopolymerization continues. Indeed, the formation of the final porous interface can be observed at longer time by Small Angle X-ray Scattering [5].

In this mechanism, the water behaves as a reactive medium. A study of paramagnetic electronic resonance followed the behavior of water during the reaction [5]. Results indicate that the water is consumed during the dissolution and hydrolysis step, and is regenerated during the poly-condensation step.

We can note that in parallel with this polymerization, nucleation-crystallization phenomenon can occur under some experimental conditions and/or with exotic formulations. Thus, the structure globally amorphous can also contain crystalline phases.

2.2 Structure and properties of geopolymers

Physical and chemical properties of geopolymers such as mechanical strength, durability and permeability are induced by its microstructure. However, the geopolymer microstructure is strongly dependent of its formulation. Modifying the relative quantity of silica, alumina, alkali ions, and water, geopolymers with various structural properties can be synthesized.

Some general rules are presented here and detailed in the next section (2.3) as a function of the formulation parameters.

2.2.1 Structure

The geopolymer structure is amorphous and composed of aluminate and silicates tetrahedrons. All those species are tetra coordinated. This implies that two aluminates cannot be directly linked by a hydrogen bond with respect to the Loewenstein avoidance rule in aluminosilicates as this would be energetically unfavorable [16,17]. Thus, the Si/Al ratio should always be greater than 1. Indeed, for low Si/Al ratio, an NMR study concluded that some Al-O-Al bonds can be present [2] and the relatively low stability of this bonds must be considered, especially for the use of geopolymers as durable, and chemically resistant binders in high-risk applications including immobilization of toxic and/or radioactive wastes

As tetra-coordinated aluminates present a negative charge, alkali ions are present in the structure to balance the electric charge and preserve the electro neutrality of the system. Those cations are believed to be hydrated in the structure, with a hydration sphere depending on the element selected (Na, K, Rb or Cs). A representation of the structure of a sodium-based geopolymer is presented on Figure 2. With respect to this stoichiometry, the molar ratio M/Al (M = Na, K, Rb or Cs) is usually equal to 1 in the geopolymer formulation.

2.2.2 Porosity

The porosity of geopolymers has been the subject of numerous papers, discussions and a Ph.D. thesis [13,18–26]. According to these studies, geopolymers can be either mainly macroporous, mainly mesoporous or mainly microporous. The most complete study was performed by V. Bénavent using many technics allowing characterizing the geopolymer porosity (nitrogen and water adsorption, small angle X ray and neutron diffusion, mercury intrusion, ions diffusiometry, TEM). This study shows that geopolymer are mainly macro and mesoporous with a proportion that varies essentially with the amount of water in the formulation. As these results are recent, (October 2016) an international consensus is yet to find.

However, most authors agree that metakaolin based geopolymers with a non-exotic formulation and cure, have a total porous volume fraction of about 0.4 and that at least a fraction of this porosity is mesoporous.

2.2.3 Mechanical strength

The mechanical strength of a geopolymer is strongly dependent on the formulation, the cure parameters, the raw materials and potential filler or reinforcements. As Ordinary Portland Cements (OPCs) and other hydraulic binders, geopolymer pastes usually have low flexion strength without reinforcement (<5 MPa). The compressive strength however can be either low or greater than 100 MPa with the appropriate formulation and curing conditions.

2.2.4 Alkali silica reaction

The alkali-silica reaction (ASR) is a widely studied reaction involving the presence of soluble alkalis, a moist environment and the presence of alkali-reactive aggregates. In OPC concrete, this reaction causes significant and irreversible damages in structures due to swelling of the concrete. Thus, this reaction must be anticipated each time a silica containing filler is added to the paste.

However, a study of the ASR on geopolymer [27,28] showed that the incorporation of reactive sands in metakaolin-based geopolymer mortars activated by sodium silicate does not lead to the ASR swelling characteristic of OPC mortars. If this study demonstrated that the durability of the geopolymer against ASR

could be higher than that of OPC under the same test conditions, it did not demonstrate that the ASR does not occurs in geopolymers.

2.2.5 Carbonation

The carbonation phenomenon in OPC pastes is known to be a slow reaction of dissolution of CO_2 in the pore solution. It leads to the formation of insoluble calcium carbonate deeper and deeper in the structure. The consequence of this carbonation is a gradual decrease in the pH of the pore solution. The pH can reach a value lower than 9, which is the limit value for the depassivation of steel in concrete, and can induce corrosion phenomena. In geopolymer based on metakaolin having a very low calcium content, dissolved CO_2 reacts with the abundant alkalis in the pore solution to form alkali-carbonates. It has been shown [27,29–32] that alkali carbonates are formed but the high solubility of these carbonates and their pH greater than 10 induce different consequences for geopolymers. The carbonation is a lot faster for geopolymers (pore solution carbonated at 97% in 14 days), the risk of corrosion by carbonation in metakaolin-based geopolymer activated is negligible and only an increase in the CO_2 content of the air, or a significant increase in temperature would lead to durability issues due to carbonation.

However, if the geopolymer is partially immerged in water, inducing a mono-directional capillary flux in the sample, efflorescence phenomenon can occur [27]. This phenomenon is defined as the significant growth of carbonate crystals on the surface of the sample, leading to notable aesthetic problems and potential surface damages.

2.2.6 Acid resistance

In the literature, geopolymers are known to conserve their structural integrity when exposed to an acidic medium. Most of the studies on this subject have been performed on fly ash based geopolymers and results can vary from an excellent resistance to the acidic attack [33,34] to a partial degradation of the structure [35–37]. The fly ash used is different in those studies and there is little information in the literature on metakaolin-based geopolymers. Thus, the reason for the satisfactory acid resistance of geopolymer remains unclear. One article [38] studied the behavior of metakaolin based potassium geopolymer under in HCl solution in different scenarios and concentrations. The geopolymers structure and mechanical properties always remained intact. However, a considerable amount of potassium was released, likely due to the exchange of K^+ ions in the geopolymer structure with H^+ ions in the solution.

2.2.7 Thermal resistance

Geopolymers usually exhibit remarkable thermal stability when properly cured. After losing their hydration water between 80 and 200 °C, they retain their X-ray-amorphous tetrahedral Al and Si network up to high temperatures. Over 800 °C, crystalline phases are formed, and the main crystalline nature of those phases depends on the cation selected in their formulation. Nepheline is formed for sodium geopolymers [39,40], leucite [39] for potassium geopolymers and pollucite [40,41] in presence of cesium. They finally melt around 1100~1200 °C.

Their thermal expansion or shrinkage, and thus the formation of cracks or micro-cracks strongly depend on the cation selection, cure parameters and the addition of a filler. With cesium geopolymers, the

dimensional and refractory properties of the geopolymer concrete can be excellent [40] making cesium geopolymers good candidates for high end refractory applications.

2.2.8 Temporal evolution and durability

Geopolymers are still a recent material, and metakaolin based geopolymer utilization in the many "clinker-free cement" constructions currently under way in the world with alkali-activated materials remains marginal. Studies have been carried out on the early-age evolution of geopolymers, but long-term evolution is still subject to discussion.

With non-exotic formulation and raw materials, the setting of geopolymers is measured between a few minutes and a few hours at ambient temperature. The material then continues to evolve fast and reaches about 80% of its final compressive strength in a few hours or days [27].

Over the first months/years, a small closure of the porosity can be observed [22] along with a change in the pore solution composition [42] and a modification of the pore surface [43]. These evolutions are dependent on the cation present in the structure. As they involve dewatering, they also depend on the relative humidity of the material environment. Indeed, in the thesis of V. Bénavent [20], samples were stored in 100% humidity and nearly no evolution of the sample was observed after the first few days.

For long-term durability, because of the lack of experience with these binders, literatures on metakaolin-based systems are not conclusive concerning the potential issues of these materials. As their structure and chemistry differs from OPCs, the accelerated tests existing for OPCs may not be applicable to geopolymers [27,30,44].

2.3 Formulation

In this section, the impact of each formulation parameter will be discussed. A visual representation of the relation between formulation parameters and macroscopic properties such as paste viscosity, setting time etc. is presented on Figure 3.

2.3.1 Alkali cation

As mentioned in part 2.2.1, tetra-coordinated aluminates in the geopolymer structure present a negative charge and alkali cations are present in the structure to balance the electric charge. Usually, this cation is either Na^+ or K^+, or to a lesser extent, Rb^+ or Cs^+.

In many patents, Li^+ and Fr^+ are also cited as potential activators respectively but are scarcely and never used in the literature. Indeed, lithium cannot be used to obtain a lithium aluminosilicate without a cure or treatment at high temperature because of its low reactivity [45–47]. Francium is never used for obvious safety, price and availability reasons.

2.3.1.1 Impact on activating solution

The impact of the nature of the alkali cation was studied in the thesis of P. Steins [48]. It was shown that when alkali cation size increases ($Na^+ \rightarrow K^+ \rightarrow Cs^+$) the silica connectivity, oligomers species size and interactions between silicate species become more important. This induces different behavior with the Si/M

molar ratio in the activating solution (M=Na, K, or Cs). For example, gelification phenomena was observed for lower Si/Al ratios for potassium activating solution compared to sodium based activating solutions.

These differences in terms of silicate speciation in the solution can also be used to explain the disparities in reactivity and geopolymer structuration observed according to the cation used and developed in the next parts.

2.3.1.2 Impact on reactivity

The network percolation time was measured for the same geopolymer formulation but different alkali ion either rheologically [5,15,48] or by in situ energy-dispersive X-ray diffractometry [49]. It was found that when alkali cation size increased ($Na^+ \rightarrow K^+ \rightarrow Cs^+$) the geopolymerization rate decreased. This phenomenon was attributed to a slower metakaolin dissolution [5]. However, even if the time needed for the paste to create a first percolating network is different for each cation, the activating energy of the geopolymerization is not strongly modified. Indeed, Poulesquen et al. [15] repeated the rheological investigation on K and Na based geopolymer at various temperature to estimate the activation energy of the reaction by plotting an Arrhenius diagram. The activation energy thus calculated is equal to 74.5 kJ/mol and 64.8 kJ/mol respectively for Na and K based geopolymers. Those close values suggest that the reaction mechanism is similar for different cation even if the reaction times differ.

2.3.1.3 Impact on geopolymer porosity

All studies about the impact of the nature of the cation in geopolymers [13,18,20,23,48,50] affirm that geopolymers with bigger size cations have a smaller and narrower pore size and thus a higher specific surface. An example of this effect extracted from thesis of P. Steins Ph.D. is presented in Table 1. This can be tentatively explained by the silicates and aluminosilicate species speciation. With larger oligomers, the reorganization of the matrix before the percolation of the geopolymer network is different. The reduction of the mobility of the geopolymer precursors limits the coalescence of pores, leading to the formation of smaller pores.

2.3.2 M/Al ratio (M = Na, K or Cs)

The alkaline hydroxide amount plays an important role in the geopolymerization process. For the same alkali cation, the dissolution of the aluminosilicate source will be faster if the activing solution pH is higher [51]. Rees et al. studied the relation between the sodium hydroxide concentration and geopolymerization through an in situ FTIR measurement [52] (with fly ashes). It was observed that the geopolymerization rates initially increase up to a maximum (in this case Na/Al = 0.63) and slightly decrease for higher sodium hydroxide concentrations. They attributed the decrease to the formation of ions pair. Thus, the position of the maximum may also depend on other parameters of the formulation. We must note that in this study as the Na/Al ratio is modified, the final material may differ for each experiment.

Wang et al. [53] performed a similar experiment with a metakaolin based geopolymer, but focusing on the mechanical strength of the obtained material. They kept every formulation ratio nearly constant except Na/Al. The modification of the latter was obtained by the addition of the same volume of NaOH solutions with different concentrations to each activating solution. Results clearly indicate that a higher Na/Al ratio allows reaching higher mechanical strength and density. As stated in part 1.3.1, this ratio is usually fixed at

1 to respect the stoichiometry of the geopolymer structure, it would thus be interesting to know which formulation of this publication corresponds to this ratio. Unfortunately, the Na/Al ratio is not stated by authors.

Finally, the M/Al ratio also induces modifications of the leaching properties of the geopolymer. Kuenzel et al. [54] performed leaching experiments for Na and K metakaolin based geopolymers. The M/Al ratio was fixed at 0.7, 1 or 1.3. Their results show an increase of the amount of leached cations with the increments of the Na/Al ratio.

2.3.3 Si/Al ratio

As mentioned in part 2.2.1, to respect the Loewenstein avoidance rule in aluminosilicates the Si/Al ratio should be greater than 1. The structure of geopolymers was studied by White et al. [55]. The samples were synthesized either with an activation by a NaOH solution (Si/Al =1) or by a water glass solution (Si/Al = 2). Samples were analyzed by pair diffraction analysis (PDF) after 90 days of curing. The comparison of the obtained pair distribution functions showed that the sample with Si/Al = 1 has a more ordered structure at a molecular scale. This result thus indicates that an addition of silica in the structure inhibits the formation of crystalline phases.

The impact on geopolymerization and geopolymer structure of the silicates speciation in the activating solution was already treated is the previous part as the alkali cation play an important role in this speciation. Many studies showed that the concentration of silica in this solution also modifies the silica speciation and that the repercussions are similar to the ones previously mentioned. An increase of the Si/Al ratio induces an increase of the oligomers size and thus a decrease of reactivity, a diminution of the pore size, and an increase of the mechanical strength and vice versa.

However, if the Si/Al ratio is too important, a gelification phenomenon will occur causing a decrease of reactivity and inducing a non-total dissolution of the metakaolin. In fact, an optimum in terms of mechanical strength is usually found with a Si/Al ratio around 1.9.

2.3.4 Water content

The effect of the water content was studied by Barbosa et al. [56] with molar ratios H_2O/Na_2O between 10 and 25. Na/Al and Si/Al ratio were respectively fixed at 0.825 and 1.65. It was shown that higher water contents induce lower reactivity and mechanical strength. Geopolymers with the higher water content needed 24 hours to harden and had extremely low mechanical strength.

With similar formulations, in the thesis for Ph.D. of A. Bourlon [12], the viscosity of the activating solution was measured. It was shown that this viscosity decreases on more than one order of magnitude. An optimum between the rheological properties of the paste, its reactivity and the mechanical strength of the geopolymer must thus be found. Usually, this maximum is found with H_2O/Na_2O ratios between 9 and 14.

During her Ph.D., V Bénavent [20] studied the porosity and properties of geopolymers with various formulations and with H_2O/Na_2O ratios between 11.5 and 13. Although the macroscopic properties were comparable on this small range, it was shown than even a small increase of the water content induce a consequent increase of the pore size and a different repartition of the water between macro-pores and

mesopores. Indeed, by DSC, it is possible to confirm that a larger water content induces a larger proportion of unconfined water present in macro-pores.

2.3.5 Raw materials

Even focusing on pure pastes of metakaolin-based geopolymers, the selection of the raw material should be done carefully. Indeed, some studies showed that different properties and reaction times can be obtained for the same formulation.

Metakaolin is obtained by the application of a thermal treatment on kaolinite above 750 °C. There are many ways to perform this treatment which are seldom detailed by metakaolin suppliers. They lead to metakaolins with different amorphous ratios, grain size and specific surface. As the kinetic of geopolymerization depends on the metakaolin dissolution rate, these parameters affect the process of geopolymerization. A striking example of this phenomenon is exposed in a study of Autef et al. [57]. In this publication, the same kaolinite was dehydrated at the same temperature (750 °C) by three different means:

• In an oven
• In a rotary furnace
• By flash dehydration

Every metakaolin obtained is different in terms of amorphous content and specific surface. The kinetic of the geopolymerization was followed by in-situ FTIR and the trends clearly indicate that a higher amorphous content and specific surface induce a faster geopolymerization.

Moreover, San Nicolas et al. [58] and Favier et al. [59] studied the impact of the metakaolin on the paste viscosity and showed that different metakaolin could induce different paste behaviors. Thus, the aluminosilicate source must be selected carefully.

2.4 Unascertained or unexplored

Although many studies have already been performed on pure geopolymers, some questions are still waiting for an answer or an international agreement. The durability of geopolymers for example is still discussed. As the geopolymer structure differs from the one of cementitious materials, new tools to predict the lifespan of geopolymer should be found.

Moreover, if the geopolymer is used as a coating or is in direct contact with another material, interactions are difficult to predict. For example, if a geopolymer is in contact with OPCs, calcium may migrate from the OPC. The excess of calcium in OPCs and the leachable silica of geopolymers might induce the formation of CSH phases (calcium silicate hydrates). It would be interesting to study this phenomenon as it could damage, or on the contrary reinforce one or both binders.

Another point remains vague in the literature. The amount of hydroxide ions and alkali cations were always modified simultaneously. The kinetic was determined for many NaOH concentrations but not the activation energy of the reaction. Moreover, the ionic force of the solution was never compensated. Thus, we cannot predict the effect of the substitution of a portion of the hydroxide by another alkaline salt. This question might be interesting to answer in the hypothesis of the addition of a filler containing sodium chloride or exchangeable Cs for example.

3. Geopolymer composites

3.1 Sand and aggregates

Sand and aggregates are usually added to OPCs and other clinker based binders. These additions allow reducing the cost, the shrinkage, and the water content and increasing the frost resistance of the material. Thus, it was natural to investigate the properties of geopolymer-based mortars (binder + sand) and concretes (binder + sand + aggregates).

C. Kuenzel et al. [60] synthesized metakaolin based mortars with silica sand at various incorporation ratios and various water content. They studied the viscosity of the paste as a function of the sand volume fraction and the influence of the incorporation ratio on mechanical strength and the mortar behavior at high temperature (up to 600 °C).

They showed that higher water content allowed a higher incorporation ratio, up to 40% in volume in their study. The evolution of the viscosity of the paste/slurries as a function of the metakaolin of sand volume fraction was followed rheologically. They could show that metakaolin particles are more detrimental in terms of viscosity than the sand. As mentioned in part 2.3.5, the type of metakaolin selected also plays an important part in the paste viscosity. Thus, a high water content and an appropriate metakaolin allow reaching higher solid particles volume fraction. Although it is unclear if the sand addition enhances the mechanical strength at ambient temperature, the behavior when exposed to high temperature is clearly modified. Indeed, the shrinkage is significantly reduced and the mortars with more than 10 % in volume of sand showed no cracks after a thermal treatment at 600 °C.

This result shows that the presence of sand or aggregates allows the binder to withstand an internal stress. Pouhet et al. [61] suggested that this excellent behavior of geopolymers concretes could be due to the absence of interfacial transition zone between the geopolymer matrix and the filler. Other studies incorporated sand and/or aggregates in geopolymers with an applicative point of view and gave similar results [62–66].

3.2 Inorganic fibers (non metallic)

Like in other binders, it can be interesting to add inorganic fiber to geopolymers. In the literature, various inorganic fibers were incorporated in geopolymers such as SiC fibers [67,68], basalt fibers [69], carbon fibers [70–76] and refractory fibers [77,78].

These fibers allowed increasing the bending strength of the material even at high temperature. This increase depends strongly on the nature, amount and length of the fiber. It is thus complicated to predict the enhancement of the mechanical properties for a given geopolymer/fiber composite. Composites with short fibers can also exhibit a non-catastrophic breaking behavior. Moreover, carbon fibers can also increase the electrical conductivity of the obtained material.

Only SiC fibers were found to interact with the geopolymerization, increasing the setting time. For every other inorganic fiber, no interaction was mentioned in the literature.

3.3 Organic fibers

The incorporation of organic fibers into geopolymer matrix was carried out with many different polymers. For example: Polyvynil-alcohol (PVA) [79], polyacetal (POM) [80], polypropylene (PP) [81,82], polystyrene (PS) [83] and polylactic-acid(PLA) [84,85]. Natural fiber were also incorporated in geopolymers, such as cotton [86], bamboo [87], corn husk fibers [88], wool [89] and jute [90].

The incorporation can have various goals such as:

• Reinforcement of the matrix

• Creation of an additional porosity after the removal of the fiber by chemical or thermal treatment

• Fireproofing of a fabric with a geopolymer coating

…

Like for the inorganic fibers, the incorporation of organic fibers often allows to increase the tensile strength of the material.

3.4 Metal

The addition of steel to ordinary concreate is commonly performed to enhance the material mechanical properties. In the same way, steel was incorporated in geopolymers, either as microfibers [82,91] or as bars [92–95]. Results are similar for all these publications. Like OPCs, the geopolymer passivates the surface thanks to its high pH and the presence of steel in the structure enhances the mechanical behavior of the material. In the presence of chlorides, geopolymers shows either better or similar passivating properties than OPCs.

Moreover, the geopolymer shows a strong adhesion to the steel. This is coherent with results for other applications of geopolymers out of the scope of this review such as steel coating [96–98] or geopolymer based adhesive [99,100].

4. Geopolymer solidification of nuclear wastes

In this part, the studies about geopolymers as an immobilization matrix for nuclear waste will be presented. These studies will be separated by waste nature and by country/organization for the sake of clarity. For convenience, these studies and patents with the associated references are also ordered by country in Table 2

4.1 Sludge, resin, liquid wastes and their mixtures

Slovakia and Czech Republic

Metakaolin based geopolymers, under the commercial name SIAL®, have been employed in Slovakia and Czech Republic since 2003 to immobilize sludge, resin, liquid wastes and their mixtures contaminated with ^{137}Cs.

A detailed report [101] summarize all the immobilizations performed between 2003 and 2010. Solidifications were carried out with an incorporation ratio between 12 and 17.5 wt % of dry matter of waste in the final product. Approximately 29.6 m^3 (38.15 t) of wastes with total activity around 4.94×10^{12} Bq were immobilized between 2003 and 2010.

Obtained wasteforms had sufficient leachability index and compressive strength to satisfy Slovak and Czech storage requirement, respectively 4 to 8 % and around 25 MPa. Thus, the SIAL® matrix was approved for waste package for sludge/resins mixture by the Slovak and Czech Nuclear Regulatory Authorities.

4.2 Zeolites

UK – Imperial College – DIAMOND consortium

C. Kuenzel et al. [54] investigated the encapsulation of Cs and Sr contaminated clinoptilolite (zeolite) in a metakaolin based geopolymer matrix. Their study is focused on different points:

- Chemical interactions between clinoptilolite and the geopolymer
- Effect of Cs and Sr on geopolymer matrix
- Leaching of Cs from geopolymer
- Leaching of Sr from geopolymer

The chemical interactions between the zeolite and the geopolymer were observed by SEM-EDX. The effect of Sr and Cs cations were evaluated by TGA and XRD. Leaching experiments were performed using the European standard BS EN 12457-2:2002 and leached ions were quantified by ICP-OES.

Their results indicate that the clinoptilolite is partially soluble in the geopolymer activating solution. Indeed, when a zeolite contaminated with Cs is introduced in a buffer solution at a pH over 11, dissolved silica can be observed by ICP-OES. Moreover, this dissolution causes an important leaching of Cs in the solution.

For geopolymer/zeolite composites, this dissolution leads to the formation of an interfacial transition zone between the geopolymer matrix and the encapsulated zeolite. In this zone, the chemical composition gradually evolves from the composition of one constituent to the one of the other. Thus, the elements dissolved from the zeolite are directly incorporated in the geopolymer matrix.

However, this result may not be extrapolated directly to other zeolites. H. Mimura and K. Akiba [102] studied the synthesis of zeolite P and the adsorption behavior of Cs and Sr in these materials. In this

publication, zeolite P structure was obtained by the conversion of other zeolites in a NaOH solution. They showed that zeolites with high Si/Al ratio, such as clinoptilolite and mordenite could be converted into zeolites P in that media. However, the conversion was not observed with zeolite having lower Si/Al ratios such as zeolites A, X, Y, L and chabazite. Their dissolution rate was found to be much slower than the one of siliceous zeolites such as clinoptilolite. Thus, judging from the relative stability observed by H. Mimura and K. Akiba, the dissolution of zeolites observed by C. Kuenzel may not be observed if the zeolite incorporated has a low Si/Al composition.

In the publication of C. Kuenzel, to separate the leaching of Cs from the matrix from the zeolite dissolution, CsOH was added to the geopolymer formulation up to a molar ratio Cs/Al = 0.3. The molar ratio Na or K /Al was also modified, ranging from 0.7 to 1.3. These leaching experiments revealed that sodium based geopolymers have a better selectivity for Cs, with no detectable leaching of this element for every molar ratio. Moreover, the amount of alkaline cations leached is lower for low Na or K/Al ratios. In terms of geopolymer structure, no evolution due to the presence of Cs was observed; the XRD data of these samples is that of a normal geopolymer.

As better selectivity for Cs was observed when Na is the charge-balancing ion, the Sr encapsulation experiment focused only on sodium-based geopolymers. When $Sr(OH)_2$ is added to the geopolymer formulation up to a Sr/Al molar ratio equal to 0.6, no leaching of Sr can be observed. However, this addition increases the amount of Na leached. This increase can be explained by the formation of a CSH like gel in the structure. Indeed, the presence of this type of amorphous phase was confirmed by TGA. However, XRD experiment also showed that Sr can be present in the wasteform as $Sr(OH)_2$ and $SrCO_3$ in large amount when the Sr/Al ratio is higher than 0.4. The extremely low leaching of Sr is thus also explained by the low solubility of these phases in the high pH of the geopolymer matrix.

China – Southwest University of science and technology

Recently Xu et al.[103] studied the immobilization of strontium loaded type A zeolites in a metakaolin based geopolymer. The formulation used was 1.25 Na_2O; 3.1 SiO_2; 1 Al_2O_3; 13 H_2O with a mass incorporation ratio of zeolite of about 28%. The zeolites are considered non-reactive and not included in the formulation. The compressive strength was measured after 28 days of cure at ambient temperature, after calcination at 600, 800 and 1000°C and after 15 freeze thaw cycles. The mechanical strength measured after the cure was about 38 MPa and of 33.5, 28.5 and 27 MPa after respectively the 600, 800 and 1000°C thermal treatments. After 15 freeze thaw cycles (-20°C for 3h and immersed in ambient temperature water for 4h) the mechanical resistance only dropped to 34 MPa, showing the good thermal behavior of their wasteform both at high and low temperature.

The confinement properties regarding the strontium present in the zeolites were also investigated. By SEM-EDX, they showed that most of the Sr remained in the zeolites. Leaching experiments were also performed in semi-static conditions during 42 days in deionized water, a sulfuric acid solution (pH = 1), a magnesium sulfuric acid solution (5%wt $MgSO_4$) and an acetic acid buffer solution (pH = 3.6). The amount of Sr leaching was higher in acidic conditions than in the deionized water, especially in the $MgSO_4$ solution where an ion exchange between Mg and Sr is suspected by the authors. However, consistently with

Kuenzel results presented previously, the overall amount of Sr leached remained low and lower than the ones obtained with cements in every media.

4.3 Magnox swarf – Aluminum metal

UK – Imperial College – DIAMOND consortium

The immobilization of aluminum metal in a hydraulic binder is complicated by the corrosion potential of the metal at high pH. Recent studies in French CEA, such as the thesis of Ph.D. of H. Lahalle [104], show that neutral binder such as magnesium phosphate cements are well suited for these immobilizations. However, geopolymer derived from metakaolin has been investigated as alternative encapsulation matrix for Magnox (Magnesium non oxidizing) swarf contaminated with traces of aluminum metal in the UK during the Ph.D. of C. Kuenzel [105].

The optimum pH range to encapsulate Al is at a pH below 11. C. Kuenzel showed that it is possible to decrease the pH of the geopolymer matrix by selecting the appropriate metakaolin and reducing the molar Na/Al ratio. However, it was not possible to reduce the pH enough to avoid completely Al corrosion. The "best" formulation of this study shows the formation of bayerite and gibbsite (aluminum hydroxides) at the aluminum surface. These phases act as passivation layer that reduce the corrosion down to a suitable level. However, the needed formulation adjustment to obtain these results induces long setting time and reduces the geopolymer compressive strength.

4.4 Mg-Zr alloys from UNGG reactors

France – CEA

Roose et al. [106,107] studied the incorporation of massive metallic alloys of Mg and Zr in a metakaolin based geopolymer matrix and compared the galvanic corrosion rates of these alloy in geopolymer and OPC. The results point out that sodium based geopolymers are the most suitable binder for Mg-Zr alloys toward Mg corrosion resistance and dihydrogen production.

Moreover, the absence of calcium in metakaolin-based geopolymer allows the addition of NaF to the binder formulation. Indeed, in OPC or blast furnace slag based binders, an addition of NaF would lead to the precipitation of CaF_2 because of the low solubility of this salt in water. NaF in geopolymers is found extremely interesting by the authors for the immobilization of radioactive waste. In fact, this addition allows at the same time the formation of an efficient passivating layer on the metal [108,109] and seems to reduce the dihydrogen produced by water radiolysis under gamma irradiation. It was observed by ^{19}F NMR that high contents of NaF in the geopolymer lead to the formation of SiF_4. However, as the needed concentration of NaF is low, no macroscopically observable effect of NaF was observed on the geopolymer properties.

The same team also published a patent with a different method [110]. In this patent, the metal is first completely dissolved/oxidized in a molten salt (KOH in the patent example). After this step, a reactive salt is obtained and dissolved in water. This solution, being very alkaline can be used to obtain the final waste form by activation of metakaolin. This method can be used for metallic powders or wastes with a high specific surface for which the formation of a passivating layer is insufficient.

4.5 Graphite

Germany - Institute of Energy and Climate Research – Jülich

Geopolymers might have been studied in Germany Forschungszentrum Jülich for the encapsulation of graphite in various forms. A document available on the IAEA website by N.A. Girke entitled “Cementation of nuclear graphite using geopolymers” claims that the incorporation of graphite in a geopolymer was successfully performed for powders (7 µm), granulate (1.25-4 mm) or small cylinders (1-1.5 cm) of graphite. However, the type of aluminosilicate source (metakaolin, fly ash, slags, used glass …), the composition of the activating solution, the amount of sand used and eventual additive are not given.

4.6 Salts

In addition to the studies of salt incorporation presented herein, the immobilization of Sr and Cs hydroxides salts was studied in the UK as a part of the investigation of the immobilization of clinoptilolite. These results are thus detailed in part 4.2.

Australia - Institute of Nuclear Science and Engineering

The effect of Sr and Cs salts on sodium metakaolin based geopolymers structuration was studied by J.L. Provis et al. [8]. Nitrates, sulfates or hydroxides of Cs or Sr were added to the geopolymer with an incorporation ratio ranging from 0.5 to 5 wt%. The selected formulation for the geopolymer was 1 Na_2O; 4 SiO_2; 1 Al_2O_3; 13.3 H_2O

Alternating current impedance spectroscopy (ACIS) was used to monitor in situ the kinetics of geopolymerization by alkali silicate activation of metakaolin at 40°C. XRD analysis was performed after 100 days at 40 °C and 95 % relative humidity to monitor the formation of crystalline phases caused by the salt addition.

Each of the six salts investigated has a different effect on the early stages of geopolymerization. For hydroxides, CsOH is particularly enhancing metakaolin dissolution and accelerating gel formation. $Sr(OH)_2$ added as an anhydrous salt gives an increase in gel resistivity which is believed to be associated with the removal of water from the water-poor geopolymerization medium.

Nitrates salt addition caused an important modification in the geopolymerization process. $Sr(NO_3)_2$ causes a very marked disruption to the development of the geopolymer gel pore network as evidenced by a dramatic reduction in resistivity reaction process. In fact, during the experiment with 5% in weight of $Sr(NO_3)_2$, the sample resistivity has barely increased above that of an unreacted geopolymer slurry. The same effect was observed with $CsNO_3$ but to a lesser extent. Thus, authors conclude that the presence of nitrates in consequent quantity is extremely damageable for the structuration of the geopolymer porosity.

$SrSO_4$ has relatively little effect early in the geopolymerization process due to its limited solubility. However, Cs_2SO_4 had an effect very similar to the one previous observed for $CsNO_3$.

At last, soluble or sparingly soluble strontium salts tend to be converted to $SrCO_3$ by atmospheric carbonation as geopolymerization proceeds.

Blackford et al. [111] also studied the incorporation of 5 % in weight of Sr or Cs hydroxides in a geopolymer matrix with a similar formulation. Samples were characterized by NMR and TEM to obtain the repartition of Cs and Sr in the geopolymer matrix. Results are in agreement with the one obtained by Kuenzel et al. [54] and presented in part 4.2.

Germany and Egypt – Jülich and Alexandria University

A study concerning the immobilization of intermediate level wastes in geopolymers was conducted by M.Y. Khalil and E. Merz [112]. The studied waste was a mix nitrates salts of Na, Al, Ca, Cr, Cs, Cu, Fe, K, Mg, Mn, Mo, Ni, Ru, Sr, Zn and Zr. This mix was incorporated in different binders and leaching tests were performed over 6 months either in water or in a "Q brine" solution. The latter, not defined in the publication, might be an $MgCl_2$ saturated solution.

Although leaching results are presented for 10 different binders with three different aluminosilicates sources. The composition of these aluminosilicates sources are not given and only referred as commercial names ROS, KOS and SECAR 51. Judging from the calcium content of the final wasteforms, ROS and KOS might be metakaolins or class F fly ash. SECAR 51 is high alumina cement with a higher proportion of calcium. The activating solution is either a sodium/potassium waterglass solution or a sodium water glass solution. The composition of the activating solution is known for only one sample.

Out of the 10 samples, 6 wasteform compositions are given. It is extremely complicated to analyze the results of this publication as the formulation parameters are varying simultaneously and over a wide range. The main alkali cation can be either sodium or potassium, the molar ratio M/Al (M=Na or K) can vary between 0.32 and 1.16 and the molar ratio Si/Al between 0.93 and 2.35.

The leaching result shows an important release of every element in Q-brine and of all elements except Sr in water. However, it is difficult to determine if these results are caused by the formulations, the raw material, the amount of added salts or the nature of the salt. With regard to the result obtained by Provis et al. [8] in the previous section with nitrate salts of Cs and Sr, the result of this study can only confirm that geopolymer are cannot be employed for the immobilization of nitrates if high retention performance are required.

4.7 Cobalt ($CoCl_2$)

Egypt – Atomic Energy Authority

M.R. El-Naggar [113] studied the incorporation of ^{60}Co in a metakaolin based geopolymer, or in a mix with this geopolymer and blast furnace slag. Leaching experiments were carried out on samples charged with 2% loading of $CoCl_2$ salt using the IAEA standard test proposed by Hespe [114]. Leaching tests were thus performed in static conditions with a known exposed surface area over 28 days. The amount of leached Co was determined measuring the activity present in the water with a gamma spectrometer

Samples without $CoCl_2$ were characterized by XRD, FTIR and compressive strength. Samples had reached important mechanical strength after one week (> 40 MPa). XRD reveals a partial dissolution of the metakaolin. In term of Co leaching, the fraction of the activity leached in the water is not proportional with the square root of time and stabilizes around 0.2% of the original activity. The author interpreted these results as being induced by a wash off phenomenon. However, as the solubility of $Co(OH)_2$ in water is low (3.2 mg/L), the possibility that these results are not transposable to non-static conditions cannot be excluded. Moreover, in the high pH conditions of a depository, $[Co(OH)_4]^{2-}$ and $[Co(OH)_6]^{4-}$ might be formed. Thus, the study might overestimate the properties of geopolymers for the immobilization of Co salts.

4.8 Organic liquids

France – CEA – EXOTI Project

The possibility of incorporating organic liquids in metakaolin based geopolymers was studied during V. Cantarel Ph.D. [26,115]. The process is based on the emulsification of the organic liquid in the activating solution before the metakaolin addition. At first, a screening on different organic liquids was carried out, revealing that only acidic oils are incompatible with the geopolymerization. However, this screening revealed than the addition of a cationic or nonionic surfactant was needed to obtain homogenous wasteforms with pure oils.

The properties of a wasteform charged up to 20% in volume with a simulated waste (used motor oil) were then studied. The selected formulation for the geopolymer was 1 Al_2O_3; 3.8 SiO_2; 1 Na_2O; 13 H_2O. It was find that the oil is present in the geopolymer as small droplets (radius around 10-50 μm). The presence of oil droplets in the sample induces a small loss of compressive strength (about 20%). Leaching properties were studied in semi-static condition in water stabilized at pH 7 over a month. The titration of organics leached in the water was carried out by TOC. A leaching of 0.2% of the oil contained in the sample was observed during the first 10 days. After this limit, the amount of leached organic was negligible and below the detection limit. Thus, the first leaching might be interpreted as a wash off phenomenon.

A model system with hexadecane a geopolymer reference formulation 1 Al_2O_3; 3.6 SiO_2; 1 Na_2O; 12 H_2O was selected for further studies. The structuration of the organic liquid/geopolymer structuration was studied from the mixture of the reactants to the final material. This study revealed that there is no chemical interaction between the oil and the geopolymer. Unlike in cements, oils do not modify the hardening process of the matrix. Indeed, the kinetics (chemical and mechanical) of the geopolymerization are not impacted by the presence of oil or surfactants. However, the presence of surfactant induces an increase of the paste viscosity. A compromise must be found between the surfactant quantity and the paste viscosity.

The composite structure was also studied (chemical structure, porosity of the geopolymer and dispersion of the oil) and its properties with respect to the application to the immobilization of radioactive waste. Unlike calcium silicate-based cementitious matrices, the structure of the geopolymer is not affected by the chemical nature of the organic liquids. The structure of the wasteform matrix is identical to that of a pure geopolymer of the same formulation. The organic liquid is dispersed in spherical inclusions whose radius is between 5 and 15 μm. These droplets are separated from each other and from the environment by the mesoporous network of the geopolymer. Mechanical and leaching properties were also evaluated. Simulated waste and the model composite gave similar results, validating the model selection.

4.9 Contaminated water

Japan – Yamaguchi University

Li and Ikeda [116] submitted a patent in 2015 and a publication in 2016 [117]. In these, a method is described to solidify contaminated water using a papermaking sludge fly ash (low Ca) based geopolymer. The water is directly used for the synthesis of the geopolymer. Authors stated some good retention properties for Cs and Sr in the final wasteform. This result is coherent with the one previously described for salt immobilization in a geopolymer. A similar patent, but not for nuclear waste, was submitted by Bayer in 2008 [118].

4.10 Secondary waste in Fukushima Daiichi NPS

In a paper by Meguro Y. and Sato J. [119] (in Japanese) about the solidification of radioactive wastes in activated materials, ongoing studies about the solidification wastes in a geopolymer matrix are mentioned. The targeted waste mentioned by the authors are slurries (iron co-precipitated and carbonates), zeolites and titanic absorbents. Although those studies are still ongoing and at a laboratory examination stage, results are presented as encouraging with good mechanical strength and confinement properties regarding the Cs and Sr present in those wastes.

The authors also mention the attempted utilization of the good geopolymer behavior at high temperature to immobilize nuclear waste containing ferrocyanides. Here, the geopolymer heat-resistance being used to bear a heat treatment at 500 °C after immobilization. As cyanides are decomposed at 350 °C, this treatment allows suppressing the toxicity of the wasteform. Authors confirmed that the loss of Cs contained in the waste during the treatment was about 1% and that the geopolymer retained its confinement properties regarding this element. When the same test was carried out using OPC as a confinement matrix, a consequent amount of Cs was lost during the thermal treatment, and most of Cs eluted in water leaching experiment.

4.11 Miscellaneous

Japan – Kobe steel Ltd.

To reduce the production of hydrogen of geopolymer based wasteforms, Nakayama et al. [120] patented a dehydration method. They described a two-step heating of the wasteform (around 100 °C and then around 400 °C) in order to remove the water. As the water present in geopolymer is not included in hydrates, this removal can be effected without damaging the chemical structure of the geopolymer. (see part 2.2.7)

Germany – Battelle Institute

In 1990, patent was submitted by Froehlich et al. [121]. In this patent, the wasteform is dehydrated by application of a microwave treatment. Authors stated a complete dehydration (less than 1% of initial water remain in the final material)

In the two patents above, no information is given about the material properties and its possible rehydration in depository conditions.

Japan – Taiheiyo Cement Corp

Yamada et al. [122] also submitted a patent about the immobilization of undefined contaminated waste in a geopolymer matrix. They stated a good retention of the Cs in the final matrix. However, only coal fly ash and furnace slags are cited in the patent. Thus, their matrix might contain a non-negligible amount of Ca, depending of the coal used.

USA – P&T Global Solutions, LLC

A patent was submitted by Gong et al. [123] for the low-temperature solidification of radioactive wastes. This patent covers the addition of an “enhancer” to a geopolymer matrix to increase the confinement properties of the matrix regarding some radionuclides such as ^{99}Tc and ^{129}I. This enhancer can be either a soluble salt of metal, green rust, layered double hydroxide, layered bismuth hydroxide, a zeolite or porous glass.

Malaysia – UniMAP

A patent was submitted by Hussin et al. [124] to use geopolymer as a radiation barrier. For this application, high-density fine and coarse aggregates should be added to the geopolymer. Thus, a high-density concreate is obtained. In that case, the composite rely on the filler properties and not on the geopolymer structure.

5. Geopolymer under irradiation

The behavior of geopolymer under irradiation is a recent subject of interest. This behavior is studied in 5 documents in the literature, all published after 2013. The behavior of metakaolin based geopolymers under gamma, electron and heavy ion irradiations was the subject of F. Chupin's Ph.D. thesis [23]. The behavior under gamma irradiation was also discussed in two papers by the same CEA team in previous studies [106,125]. In another paper by Deng et al. [126], the evolution the leaching properties and structure of a Class F fly ash geopolymer charged with $CsNO_3$ under gamma irradiation was studied. At last, H. Takeda et al. [127] studied the neutron absorption capability of class F fly ash geopolymers either using a conventional curing process or applying heat and pressure on the sample during its hardening. The presentation of the results contained in these documents will be structured in four parts, one for each type of irradiation.

5.1 Behavior under gamma irradiation

Chronologically, the first papers analyzing the behavior of geopolymer under gamma irradiation are the ones published by Roose et al. [106] in 2013 and Lambertin et al. [125] in 2014. The formulations used were the following: 1 Al_2O_3; 3.8 SiO_2; 1 Na_2O; x H_2O, with x = 11, 12 or 13.

In the first paper, the irradiation was performed on a sample with a molar ratio of water equal to 11 and stored under air before the analysis. Upon gamma irradiation at 600 kGy/h under argon, the hydrogen radiolytic yield measured were low, about 6×10^{-9} mol/J after a dose of 50 kGy.

However, further studies with sealed samples, protected from dehydration, showed that this value could not be used to predict the amount of hydrogen generated by water radiolysis in storage conditions. Indeed, in the second paper, the dihydrogen production radiolytic yields in the same conditions are of 0.90×10^{-8}, 1.02×10^{-8} and 1.13×10^{-8} mol/J respectively for water molar ratios of 11, 12 and 13. Those values are still low compared to the radiolytic yield of pure bulk water but higher than the one of a partially dehydrated sample. This showed the importance of the water content of the geopolymer matrix and of the sample preparation.

In this second paper, the effect of gamma irradiation on the geopolymer structure was investigated. In terms of compressive strength, an increase of about 10% was observed after exposition up to a dose of 1 MGy. The porosity evolution was also studied, after 1MGy, an enlargement of the porosity was observed. Indeed, non-irradiated samples had a mono-modal pore size centered on 7 nm, and irradiated sample had a pore size ranging from 10 to 50 nm. Finally, in terms of structure, the samples were characterized by PDF analysis. Even after a dose of 1 MGy of gamma irradiation, the pair distribution function does not display any important changes. Indeed, only a slight shift decrease of the Si-O-Si bridging bond can be observed. Thus, it was concluded that gamma irradiation induces a slight densification of the geopolymer but does not modify strongly the amorphous structure of the geopolymer.

After these studies, the PhD of F. Chupin started with two main objectives:

• Understanding the phenomena controlling the dihydrogen production

• Evaluating the relation between the geopolymer formulation and the geopolymer behavior under irradiation.

These two objectives were pursued simultaneously. To do so, geopolymers were synthesized with different cations (Na, K or Cs), different water content and different Si/Al ratio. They were stored under

different conditions before gamma irradiation at low or high dose rate (respectively about 0.5 and 5 kGy/h). As the evolution of the structure of geopolymer as a function of all these parameters is known (see part 2.3) the main phenomena governing the hydrogen production can be deducted. According to the results, the main phenomenon affecting the hydrogen production is a coupled effect of its porosity (pore size and specific surface) and of the chemical nature of geopolymers (mean atomic number). After the inelastic scattering of a gamma ray photon by a charged particle in the material (known as Compton scattering), an energy transfer may occur via secondary electrons or excitons to the solid/interstitial interface and be responsible for an increase in dihydrogen production yields measured. These effects can be increased by two parameters as observed in this thesis:

• A small pore size and a high specific surface, inducing a larger proportion of water impacted by the transfers,

• A high mean atomic number as the number of possible interactions with electrons and excitons is then higher.

Indeed, the hydrogen production was found to be proportional to the mean atomic number of the geopolymer matrix (modified by selection of different charge balancing cations in the formulation) and inversely proportional to the pore size of the geopolymer.

With the same formulation, H_2 production yields of 1.3×10^{-8}, 2.5×10^{-8} and 4.8×10^{-8} mol/J respectively for sodium, potassium and cesium based geopolymers under gamma irradiation.

As can be inferred comparing the two first studies of this part, the water content is also an extremely important factor governing the dihydrogen production. Indeed, a perfect proportionality was observed between the dihydrogen production and the water content of the geopolymer.

In repository condition, geopolymer will be stored at 100% relative humidity. To modify the water content in these conditions, the only possibility is to modify the water molar ratio in the formulation. However, as stated in part 2.3.4, increasing this ratio will also increase the pore size in the geopolymer, and thus reduce the specific surface and the water radiolysis induced by Compton effect and vice versa. In fact, the results of F. Chupin show that for water ratios between 11 and 13 and all other parameters unchanged, the dihydrogen production yields under gamma irradiation are nearly identical. The reduction of the Compton effect importance nearly compensates the increased amount of water in the matrix.

At last, an effect of the dose was observed and linked to a dioxygen consumption. Indeed, at high doses, a high quantity of dihydrogen is formed and favorites the water recombination like in Allen type chain reaction. Thus, the hydrogen production reaches a plateau. This phenomenon is highly visible for irradiations in air with a very low dihydrogen production and a dioxygen consumption. This phenomenon may not be observed in natural conditions if the accumulation of dihydrogen is not possible, however, it enlighten the importance of the irradiation atmosphere. The geopolymer behavior was also studied. No consequent evolution of porosity was noticed for gamma irradiation up to high doses. In fact, the evolution that was attributed in the paper of Lambertin et al. [125] to the irradiation was maybe in fact due to the condition of geopolymer aging. No modification of the geopolymer structure was observed. However, PDF analysis was not carried out by F. Chupin so small modifications of the amorphous structure cannot be excluded.

Mechanical strength always remains higher than the safety criteria defined by the ANDRA (French national agency for the treatment of nuclear wastes) for immobilization matrixes, even for gamma

irradiation up to 9 MGy. The increase observed by Lambertin et al. [125] after 1 MGy is also observed by F. Chupin. However, the compressive strength returns and stabilizes around its original value after 3 MGy.

In addition to the previous studies, Deng et al. [126] submitted class F fly ash based geopolymer wasteform containing $CsNO_3$ to gamma irradiation. This study aimed at determining the effect of irradiation on Cs leaching in water, simulated ground water and simulated seawater. The effect of irradiation on porosity was also checked by mercury intrusion.

The formulation of the geopolymer is not given and the CaO content of the "Class F fly ash" is high (8.89% in weight). However, we know that $CsNO_3$ was added to this binder up to 2% in mass and that leaching tests were performed in semi-static conditions. Contrary to the addition of Cs hydroxide, when Cs nitrate is added to the geopolymer, a different porosity and Cs leaching out the geopolymer matrix can be observed. The results are coherent with the results presented in part 4.6.

All samples leaching followed a diffusion behavior. The leaching indexes were always higher than 8.7, showing a satisfying retention of Cs. Although the Cs leaching mainly depends on the leaching medium, irradiation induced a small increase of the amount of Cs leached in every leaching medium. Indeed, the diffusion coefficient was multiplied by a factor 2 after irradiation. Results for every medium before and after irradiation are presented in Table 3.

5.2 Behavior under electron irradiation

Two series of irradiation with electron beam were carried out during F. Chupin Ph.D. thesis. The first one with a continuous beam at a dose rate between 0.4 and 20 MGy/h and a dose between 0.5 and 301 MGy. The second one was carried out with a pulsed beam. The dose per impulsion was around 30 Gy, at a 10 Hz frequency and for a total deposited dose between 15 and 45 kGy. Experiments with the continuous beam were performed to study the effect of the linear energy transfer (LET) and of a potential effect of the dose rate and dose on the formation of crystalline phases in the geopolymer. Irradiation using a pulsed electron beam aimed at characterizing the created defects and the formed radicals.

5.2.1 Structural modifications

Samples were characterized by XRD after electron irradiation. On the obtained diffractograms, no crystallization can be observed. The diffractograms remained identical for every dose and dose rate. However, samples were not analyzed by PDF and small modifications of the amorphous structure cannot be excluded.

The samples were also characterized by gas adsorption and, once again, for every dose or dose rate, the porosity remained unmodified by the irradiation.

5.2.2 Creation of radicals

The creation of radicals was observed by ESR during pulsed beam irradiations. These irradiations were performed either at ambient temperature, to check the formation of stable radical species, or in liquid nitrogen, to slow down the recombination phenomenon and observe all created radicals. At low temperature, the samples are irradiated up to 17.5, 35 or 52.5 kGy at 77K (-196 ºC). ESR spectra are then recorded at 100, 120, 140 or 170 K (-173, -153, -123, -103 ºC).

At ambient temperature, no radicals can be observed by ESR up to a dose of 360 kGy. The author concluded that there were no stable radicals created under electron irradiation.

At low temperature, three types of signals can be observed by ESR. The first one, is a hyperfine coupling doublet with a constant equal to 506 Gauss (50.6 mT) centered at g = 2.013 corresponding to trapped H• radicals. The second one is a large asymmetric signal centered at g = 2.017 composed of several structures superposed and attributed to Si-O•/h^+ and Al-O•/h^+ defects. However, due to the large width of the signal, the presence of peroxide radicals cannot be excluded (for example Si-O-O•). The last signal observable is a sharp peak present at g = 1.997. It is attributed to the presence of an electron trapped in the geopolymer network. It could be a F* center, i.e. an oxygen vacancy which trapped an electron.

The intensity of every signal does not vary as a function of the dose. The created species are very reactive and recombine quickly, even at low temperature. Thus, only species present at a quasi-stationary concentration in the matrix are observed.

5.3 Behavior under heavy ion irradiation

Geopolymers were submitted to heavy ions irradiation (^{36}Ar) in F. Chupin Ph.D. thesis to simulate the effect of alpha particles on the geopolymer. Irradiations have been carried out up to 0.5 and 1 MGy with ^{36}Ar with an energy of 75 MeV/A and up to 2 MGy with ^{36}Ar with an energy of 95 MeV/A. All the experiments were effected with a dose rate of 0.5 MGy/h.

The results obtained are differing from the one of low linear energy transfer irradiation.

5.3.1 Chemical structure evolution

To investigate the chemical structure evolution, samples were analyzed by XDR and ^{29}Si MAS NMR before and after irradiation. The XRD was used to identify the potential crystallized phases. The NMR was used to quantify them.

With sodium-based geopolymer, a crystallization is observed after 0.5 MGy. Indeed, a peak in the XRD pattern at 29° appears. This peak could indicate the formation of a structure of nepheline (N) type $Na_3K(Si_{0.56}Al_{0.44})_8O_{16}$. This peak intensity decreases for larger doses (1 and 2 MGy) and this decrease is not explained.

For potassium-based geopolymer, the same phase crystallizes but in little quantity. The author made the hypothesis that this phase was obtained because of sodium present in the metakaolin. However, after 2 MGy, a second phase, the kaliophilite ($KAlSiO_4$) was formed

For cesium-based geopolymers, a clear crystallization of pollucite was observed. However, the effect of the dose is not known as the exact dose is known for only one sample.

For every sample, the volume fraction of crystalline phases was about 2% before irradiation and about 5% after an irradiation up to 1 MGy. This clearly shows that heavy ion irradiation induces crystallization in the geopolymer structure. Moreover, the phases formed under irradiation depend on the cations present in the system.

5.3.2 Porosity evolution

The porosity evolution during the irradiation was measured by gas adsorption. A slight modification of the pore size and the formation of a small quantity of macro-pores were observed for all samples. This modification was interpreted as directly linked to the crystallizations by the author.

5.3.3 Dihydrogen production

The dihydrogen production yield was measured for various water content for sodium-based geopolymer in argon atmosphere. The yields measured vary linearly between 0.02 and 0.58×10^{-7} mol/J for water contents respectively between 1% and saturated. These yields are 4 times greater than the ones obtained during gamma experiments. This ratio is close to the one obtained with free water at a high pH (3.4). The author used this information to conclude that the water radiolysis in a sodium-based geopolymer was similar to the one observed in free water. Indeed, for high linear energy transfer irradiation, a high concentration of defects expected to be present in the matrix. This high concentration of defects leads to a high probability of recombination and reduce the probability of their migration toward the pore surface. Thus, unlike for gamma irradiation, the mean number and the specific surface do not modify the dihydrogen production yield. A schematic representation by F. Chupin of water radiolysis in geopolymer under gamma or heavy ion irradiation is presented on Figure 4 (Translated from F. Chupin Ph.D. thesis).

At last, a dose effect similar to the one observed for gamma irradiation was observed. Indeed, the dihydrogen production yield is not proportional to the applied dose. The author concluded that like during gamma irradiation, an Allen type chain reaction was occurring when a sufficient dihydrogen concentration is reached.

5.4 Behavior as neutrons absorber

Takeda et al. [124] studied fly ash based geopolymer and their ability to absorb neutrons. The formulation used is not given. Their porosity measurement showed a porosity centered on 50 μm and their compressive strength is about 20 MPa. These properties could be induced by a high amount of water. However, they also used a warm pressing curing, submitting the geopolymer paste to a pressure of 200 MPa at 130 °C for 60 minutes. In these conditions, the porosity is reduced and the mechanical strength is increased. By gas adsorption no micrometric porosity is observed and the compressive strength and density rises up to 149 MPa and 2.05 respectively.

Surprisingly, the water content measured for sample cured at high temperature is higher than the one obtained at ambient temperature. This is explained by the authors by a higher reaction extent at high temperature. This explanation is irrelevant considering the actual accepted mechanism for geopolymerization. However, samples were two years old when the water content analysis was performed. If the porosity of the cured geopolymer was smaller, the higher amount of water could be originating from capillary condensation and lower dehydration during aging or synthesis.

In terms of neutron absorption, cured and uncured two years old geopolymers were exposed to a neutron beam with an intensity of 10×10^{4} n/cm^2/s/μA. After 15 minutes of irradiation, the neutron absorption was calculated measuring the radiant gamma emission of gold filaments on both sides of the sample. Results were compared to the ones obtained for fresh or two years old OPC. The fresh OPC paste

showed the largest neutron absorption, around 4%/cm, because of the many water molecules contained in the harden body. In contrast, the neutron absorption for the aged concreate was the lowest, around 1.7%/cm. Two years old geopolymers had intermediate results, around 2.5 and 3.3 %/cm respectively for uncured and cured geopolymer. This result was explained by the authors by the higher water content of aged geopolymers.

6. Conclusions

At the present day, many studies have been performed to clarify and understand the geopolymer matrix. As we saw, this material is versatile; it is not always trivial to predict the properties and structure of a given formulation, even for metakaolin based geopolymers. It has been observed by many that geopolymers can possess interesting properties for some applications such as the immobilization of nuclear wastes. For that application, many studies and patents with different aimed wastes stated that geopolymers based wasteforms can be obtained with good mechanical strength and confinement properties. These studies are sufficient to consider the immobilization of waste with low or moderate activity as was demonstrated by the utilization of the SIAL® matrix in Europe.

Concerning nuclear wastes with a higher activity, the level of confidence required before a trial in real conditions is higher. The risks associated with the immobilization must be predicted carefully and on a longer time scale. Recently, studies have been carried out to understand and quantify the impact of radiations on the geopolymer structure, properties and predict the production of the hazardous dihydrogen generated by the water radiolysis. The results obtained by these studies are encouraging. However, their direct transposition in the risk assessment of a specific waste is not trivial. Thus, efforts are needed to understand and predict the coupled interaction between the waste and the geopolymer and quantify their influence on the risks associated with the immobilization of a defined waste.

In the specific case of the secondary wastes generated after the Fukushima accident, unique interactions are to be considered. As an example, due to the emergency of the situation, seawater was employed as a cooling solution just after the accident before being decontaminated using zeolites. Studies have already been performed to understand the hydrogen production of those wastes in their actual state [128–130] and to assess the risk associated with their storage [131]. However, specific studies are needed to predict the impact of the immobilization of this unique type of waste in a geopolymer matrix.

At last, ideas of wasteform post treatment, such as dehydration by thermal treatment, have been made and patented with the intention of reducing or even canceling the production of dihydrogen by the water radiolysis. Unlike most hydraulic binders, geopolymers could retain satisfying mechanical and chemical properties [132]. Sharing the same goal, utilization of dihydrogen mitigation catalysts or hydrogen chemical traps could also be could be efficient to reduce the dihydrogen production of geopolymer-based wasteforms. Although those ideas are appealing, studies are still needed to attest their feasibility and consequences in realistic conditions.

References

[1] Davidovits, J., Geopolymers, J. Therm. Anal., vol. 37, No. 8, 1991, pp. 1633–1656.

[2] Provis, J.L., Modelling the formation of geopolymer, University of Melbourne, 2006, thesis.

[3] Rowles, M.R. et al., ^{29}Si, ^{27}Al, ^{1}H and ^{23}Na MAS NMR Study of the Bonding Character in Aluminosilicate Inorganic Polymers, Appl. Magn. Reson., vol. 32, No. 4, 2007, pp. 663–689.

[4] Autef, A. et al., Role of the silica source on the geopolymerization rate: A thermal analysis study, J. Non-Cryst. Solids., vol. 366, 2013, pp. 13–21.

[5] Steins, P. et al., Structural Evolution during Geopolymerization from an Early Age to Consolidated Material, Langmuir, vol. 28, No. 22, 2012, pp. 8502–8510.

[6] Provis, J.L. et al., Geopolymerisation kinetics. 2. Reaction kinetic modelling, Chem. Eng. Sci., vol. 62, No. 9, 2007, pp. 2318–2329.

[7] Babushkin, V.I. et al., Thermodynamics of silicates, Springer-Verlag, 1985.

[8] Provis, J.L. et al., Geopolymerisation kinetics. 3. Effects of Cs and Sr salts, Chem. Eng. Sci., vol. 63, No. 18, 2008, pp. 4480–4489.

[9] Fernández-Jiménez, A. et al., Microstructure development of alkali-activated fly ash cement: a descriptive model, Cem. Concr. Res., vol. 35, No. 6, 2005, pp. 1204–1209.

[10] Duxson, P. et al., The thermal evolution of metakaolin geopolymers: Part 2 – Phase stability and structural development, J. Non-Cryst. Solids., vol. 353, No. 22-23, 2007, pp. 2186–2200.

[11] Rees, C.A. et al., The mechanism of geopolymer gel formation investigated through seeded nucleation, Colloids Surf. Physicochem. Eng. Asp., vol. 318, No. 1-3, 2008, pp. 97–105.

[12] Bourlon, A., Physico-chimie et rhéologie de géopolymères frais pour la cimentation des puits pétroliers, Université Pierre et Marie Curie, 2010, thesis (in French).

[13] Duxson, P. et al., Understanding the relationship between geopolymer composition, microstructure and mechanical properties, Colloids Surf. Physicochem. Eng. Asp., vol. 269, No. 1-3, 2005, pp. 47–58.

[14] Duxson, P., The structure and thermal evolution of metakaolin geopolymers, University of Melbourne, 2006, thesis.

[15] Poulesquen, A. et al., Rheological behavior of alkali-activated metakaolin during geopolymerization, J. Non-Cryst. Solids., vol. 357, No. 21, 2011, pp. 3565–3571.

[16] Massiot, D. et al., Topological, Geometric, and Chemical Order in Materials: Insights from Solid-State NMR, Acc. Chem. Res., vol. 46, No. 9, 2013, pp. 1975–1984.

[17] Loewenstein, W., The distribution of aluminum in the tetrahedra of silicates and aluminates, Am. Mineral., vol. 39, No. 1-2, 1954, pp. 92–96.

[18] Bell, J.L. et al., Nanoporosity in Aluminosilicate, Geopolymeric Cements, Microsc. Microanal., vol. 10, No. S02, 2004, pp. 590–591.

[19] Maitland, C.F. et al., Characterization of the pore structure of metakaolin-derived geopolymers by neutron scattering and electron microscopy, J. Appl. Crystallogr., vol. 44, 2011, pp. 697–707.

[20] Bénavent, V., Caractérisation de la porosité des géopolymères: Evolution temporelle et étude de l'eau confinée, Université de Montpellier, 2016, thesis (in French).

[21] Kriven, W.M. et al., Effect of Alkali Choice on Geopolymer Properties, 28th Int. Conf. Adv. Ceram. Compos. B Ceram. Eng. Sci. Proc., 2008, pp. 99–104.

[22] Steins, P. et al., Effect of aging and alkali activator on the porous structure of a geopolymer, J. Appl. Crystallogr., vol. 47, 2014, pp. 316–324.

[23] Chupin, F., Caractérisation de l'effet des irradiations sur les géopolymères, Université Pierre et Marie Curie, 2015, thesis (in French).

[24] Provis, J.L. et al., Geopolymers: Structures, Processing, Properties and Industrial Applications, Elsevier Science, 2009.
[25] Boher, C., Etude expérimentale et modélisation de la diffusion gazeuse à travers des milieux poreux partiellement saturés en eau. Application aux verres Vycor, géopolymères et pâte de ciment CEM V, Institut national des Sciences Appliquées de Toulouse, 2012, thesis (in French).
[26] Cantarel, V., Etude de la synthèse de composites liquides organiques/géopolymères en vue du conditionnement de dechets nucléaires., Université Blaise Pascal, 2016, thesis (in French).
[27] Pouhet, R., Formulation and durability of metakaolin-based geopolymers, Universite Paul Sabatier Toulouse III, 2015, thesis (in French).
[28] Pouhet, R. et al., Alkali-silica reaction in metakaolin-based geopolymer mortar, Mater. Struct., vol. 48, No. 3, 2015, pp. 571–583.
[29] Bakharev, T. et al., Resistance of alkali-activated slag concrete to carbonation, Cem. Concr. Res., vol. 31, No. 9, 2001, pp. 1277–1283.
[30] Bernal, S.A. et al., Accelerated carbonation testing of alkali-activated binders significantly underestimates service life: The role of pore solution chemistry, Cem. Concr. Res., vol. 42, No. 10, 2012, pp. 1317–1326.
[31] Bernal, S.A. et al., Effect of silicate modulus and metakaolin incorporation on the carbonation of alkali silicate-activated slags, Cem. Concr. Res., vol. 40, No. 6, 2010, pp. 898–907.
[32] Criado, M. et al., Alkali activation of fly ashes. Part 1: Effect of curing conditions on the carbonation of the reaction products, Fuel., vol. 84, No. 16, 2005, pp. 2048–2054.
[33] Palomo, A. et al., Chemical stability of cementitious materials based on metakaolin, Cem. Concr. Res., vol. 29, No. 7, 1999, pp. 997–1004.
[34] Fernandez-Jimenez, A. et al., Durability of alkali-activated fly ash cementitious materials, J. Mater. Sci., vol. 42, No. 9, 2007, pp. 3055–3065.
[35] Allahverdi, A. et al., Sulfuric acid attack on hardened paste of geopolymer cements Part 1. Mechanism of corrosion at relatively high concentrations, Ceram.-Silik., vol. 49, No. 4, 2005, pp. 225–229.
[36] Allahverdi, A. et al., Nitric acid attack on hardened paste of geopolymeric cements - Part 1, Ceram.-Silik., vol. 45, No. 3, 2001, pp. 81–88.
[37] Allahverdi, A. et al., Nitric acid attack on hardened paste of geopolymeric cements - Part 2, Ceram.-Silik., vol. 45, No. 4, 2001, pp. 143–149.
[38] Gao, X.X. et al., Behavior of metakaolin-based potassium geopolymers in acidic solutions, J. Non-Cryst. Solids., vol. 380, 2013, pp. 95–102.
[39] Bell, J.L. et al., Formation of Ceramics from Metakaolin-Based Geopolymers. Part II: K-Based Geopolymer, J. Am. Ceram. Soc., vol. 92, No. 3, 2009, pp. 607–615.
[40] Bell, J.L. et al., Formation of Ceramics from Metakaolin-Based Geopolymers: Part I - Cs-Based Geopolymer, J. Am. Ceram. Soc., vol. 92, No. 1, 2009, pp. 1–8.
[41] Chlique, C. et al., XRD Analysis of the Role of Cesium in Sodium-Based Geopolymer, J. Am. Ceram. Soc., vol. 98, No. 4, 2015, pp. 1308–1313.
[42] Lloyd, R.R. et al., Pore solution composition and alkali diffusion in inorganic polymer cement, Cem. Concr. Res., vol. 40, No. 9, 2010, pp. 1386–1392.
[43] Melar, J. et al., The Porous Network and its Interface inside Geopolymers as a Function of Alkali Cation and Aging, J. Phys. Chem. C., vol. 119, No. 31, 2015, pp. 17619–17632.
[44] Sanjuan, M. et al., Concrete carbonation tests in natural and accelerated conditions, Adv. Cem. Res., vol. 15, No. 4, 2003, pp. 171–180.
[45] Yuan, J. et al., Effects of Li Substitution on the Microstructure and Thermal Expansion Behavior of Pollucite Derived from Geopolymer, J. Am. Ceram. Soc., vol. 99, No. 11, 2016, pp. 3784–3791.

[46] Wang, Y.C. et al., Novel activator for synthesis of fly ash based geopolymer, Mater. Res. Innov., vol. 18, No. S2, 2014, pp. 238–242.
[47] Nourbakhsh, A.A. et al., A Novel Method for the Formation of Lithium Aluminosilicate and Lithium Aluminosilicate-Alumina Matrix Composites by Silicothermal Reaction of Li-Geopolymers, Mol. Cryst. Liq. Cryst., vol. 577, No. 1, 2013, pp. 116–126.
[48] Steins, P., Influence des paramètres de formulation sur la texturation et la structuration des géopolymères, Université de Limoges, 2014, thesis (in French).
[49] Provis, J.L. et al., Geopolymerisation kinetics. 1. In situ energy-dispersive X-ray diffractometry, Chem. Eng. Sci., vol. 62, No. 9, 2007, pp. 2309–2317.
[50] Duxson, P. et al., Effect of Alkali Cations on Aluminum Incorporation in Geopolymeric Gels, Ind. Eng. Chem. Res., vol. 44, No. 4, 2005, pp. 832–839.
[51] Phair, J.W. et al., Effect of silicate activator pH on the leaching and material characteristics of waste-based inorganic polymers, Miner. Eng., vol. 14, No. 3, 2001, pp. 289–304.
[52] Rees, C.A. et al., In situ ATR-FTIR study of the early stages of fly ash geopolymer gel formation, Langmuir, vol. 23, No. 17, 2007, pp. 9076–9082.
[53] Wang, W. et al., Synthesis and mechanical properties of metakaolinite-based geopolymer, Colloids Surf. Physicochem. Eng. Asp., vol. 268, No. 1-3, 2005, pp. 1–6.
[54] Kuenzel, C. et al., Encapsulation of Cs/Sr contaminated clinoptilolite in geopolymers produced from metakaolin, J. Nucl. Mater., vol. 466, 2015, pp. 94–99.
[55] White, C.E. et al., Evolution of Local Structure in Geopolymer Gels: An In Situ Neutron Pair Distribution Function Analysis, J. Am. Ceram. Soc., vol. 94, No. 10, 2011, pp. 3532–3539.
[56] Barbosa, V.F.F. et al., Synthesis and characterisation of materials based on inorganic polymers of alumina and silica: sodium polysialate polymers, Int. J. Inorg. Mater., vol. 2, No. 4, 2000, pp. 309–317.
[57] Autef, A. et al., Role of metakaolin dehydroxylation in geopolymer synthesis, Powder Technol., vol. 250, 2013, pp. 33–39.
[58] San Nicolas, R. et al., Characteristics and applications of flash metakaolins, Appl. Clay Sci., vol. 83–84, 2013, pp. 253–262.
[59] Favier, A. et al., Flow properties of MK-based geopolymer pastes. A comparative study with standard Portland cement pastes, Soft Matter., vol. 10, No. 8, 2014, pp. 1134–1141.
[60] Kuenzel, C. et al., Influence of sand on the mechanical properties of metakaolin geopolymers, Constr. Build. Mater., vol. 66, 2014, pp. 442–446.
[61] Pouhet, R. et al., Formulation and performance of flash metakaolin geopolymer concretes, Constr. Build. Mater., vol. 120, 2016, pp. 150–160.
[62] Vasconcelos, E. et al., Concrete retrofitting using metakaolin geopolymer mortars and CFRP, Constr. Build. Mater., vol. 25, No. 8, 2011, pp. 3213–3221.
[63] Clausi, M. et al., Metakaolin as a precursor of materials for applications in Cultural Heritage: Geopolymer-based mortars with ornamental stone aggregates, Appl. Clay Sci., vol. 132–133, 2016, pp. 589–599.
[64] Steinerova, M., Mechanical properties of geopolymer mortars in relation to their porous structure, Ceram.-Silik., vol. 55, No. 4, 2011, pp. 362–372.
[65] Tenn, N. et al., Formulation of new materials based on geopolymer binders and different road aggregates, Ceram. Int., vol. 41, No. 4, 2015, pp. 5812–5820.
[66] Arellano-Aguilar, R. et al., Geopolymer mortars based on a low grade metakaolin: Effects of the chemical composition, temperature and aggregate:binder ratio, Constr. Build. Mater., vol. 50, 2014, pp. 642–648.

[67] Yuan, J. et al., SiC fiber reinforced geopolymer composites, part 1: Short SiC fiber, Ceram. Int., vol. 42, No. 4, 2016, pp. 5345–5352.
[68] He, P. et al., SiC fiber reinforced geopolymer composites, part 2: Continuous SiC fiber, Ceram. Int., vol. 42, No. 10, 2016, pp. 12239–12245.
[69] Rill, E. et al., Properties of Basalt Fiber Reinforced Geopolymer Composites, Strateg. Mater. Comput. Des., 2010, pp. 57–67.
[70] Lin, T. et al., Mechanical properties and fracture behavior of electroless Ni-plated short carbon fiber reinforced geopolymer matrix composite, Int. J. Mod. Phys. B., vol. 23, No. 6-7, 2009, pp. 1371–1376.
[71] Lin, T. et al., Effects of fiber length on mechanical properties and fracture behavior of short carbon fiber reinforced geopolymer matrix composites, Mater. Sci. Eng. A -Struct., vol. 497, No. 1-2, 2008, pp. 181–185.
[72] Lin, T. et al., In situ crack growth observation and fracture behavior of short carbon fiber reinforced geopolymer matrix composites, Mater. Sci. Eng. -Struct. Mater. Prop. Microstruct. Process., vol. 527, No. 9, 2010, pp. 2404–2407.
[73] Tie-song, T. et al., Thermal-mechanical properties of short carbon fiber reinforced geopolymer matrix composites subjected to thermal load, J. Cent. South Univ. Technol., vol. 16, No. 6, 2009, pp. 881–886.
[74] Vaidya, S. et al., Strain sensing of carbon fiber reinforced geopolymer concrete, Mater. Struct., vol. 44, No. 8, 2011, pp. 1467–1475.
[75] Vaidya, S. et al., Experimental evaluation of electrical conductivity of carbon fiber reinforced fly-ash based geopolymer, Smart Struct. Syst., vol. 7, No. 1, 2011, pp. 27–40.
[76] Yan, S. et al., Effect of fiber content on the microstructure and mechanical properties of carbon fiber felt reinforced geopolymer composites, Ceram. Int., vol. 42, No. 6, 2016, pp. 7837–7843.
[77] Musil, S.S. et al., Situ Mechanical Properties of Chamotte Particulate Reinforced, Potassium Geopolymer, J. Am. Ceram. Soc., vol. 97, No. 3, 2014, pp. 907–915.
[78] Bernal, S.A. et al., Performance of refractory aluminosilicate particle/fiber-reinforced geopolymer composites, Compos. Part B-Eng., vol. 43, No. 4, 2012, pp. 1919–1928.
[79] Nematollahi, B. et al., Tensile Strain Hardening Behavior of PVA Fiber-Reinforced Engineered Geopolymer Composite, J. Mater. Civ. Eng., vol. 27, No. 10, 2015.
[80] Zhao, W. et al., Fabrication, mechanical performance and tribological behaviors of polyacetal-fiber-reinforced metakaolin-based geopolymeric composites, Ceram. Int., vol. 42, No. 5, 2016, pp. 6329–6341.
[81] Ranjbar, N. et al., Comprehensive Study of the Polypropylene Fiber Reinforced Fly Ash Based Geopolymer, Plos one., vol. 11, No. 1, 2016.
[82] Ranjbar, N. et al., Mechanisms of interfacial bond in steel and polypropylene fiber reinforced geopolymer composites, Compos. Sci. Technol., vol. 122, 2016, pp. 73–81.
[83] Glad, B.E. et al., Polymer Adhesion to Geopolymer via Silane Coupling Agent Additives, J. Am. Ceram. Soc., vol. 95, No. 12, 2012, pp. 3758–3762.
[84] Okada, K. et al., Capillary rise properties of porous geopolymers prepared by an extrusion method using polylactic acid (PLA) fibers as the pore formers, J. Eur. Ceram. Soc., vol. 31, No. 4, 2011, pp. 461–467.
[85] Rasouli, H.R. et al., Fabrication and properties of microporous metakaolin-based geopolymer bodies with polylactic acid (PLA) fibers as pore generators, Ceram. Int., vol. 41, No. 6, 2015, pp. 7872–7880.
[86] Alomayri, T. et al., Synthesis and mechanical properties of cotton fabric reinforced geopolymer composites, Compos. Part B-Eng., vol. 60, 2014, pp. 36–42.

[87] Sa Ribeiro, R.A. et al., Geopolymer-bamboo composite - A novel sustainable construction material, Constr. Build. Mater., vol. 123, 2016, pp. 501–507.
[88] Musil, S.S. et al., Green Composite: Sodium-Based Geopolymer Reinforced with Chemically Extracted Corn Husk Fibers, Dev. Strateg. Mater. Comput. Des. IV, 2013, pp. 123–133.
[89] Alzeer, M et al., Synthesis and mechanical properties of new fibre-reinforced composites of inorganic polymers with natural wool fibres, J. Mater. Sci., vol. 47, No. 19, 2012, pp. 6958–6965.
[90] Sankar, K. et al., Sodium Geopolymer Reinforced with Jute Weave, Dev. Strateg. Mater. Comput. Des. V, 2014, pp. 39–60.
[91] Bhutta, A. et al., Pull-out behavior of different fibers in geopolymer mortars: effects of alkaline solution concentration and curing, Mater. Struct., vol. 50, No. 1, 2017.
[92] Monticelli, C et al., A study on the corrosion of reinforcing bars in alkali-activated fly ash mortars under wet and dry exposures to chloride solutions, Cem. Concr. Res., vol. 87, 2016, pp. 53–63.
[93] Badar, M.S. et al., Corrosion of steel bars induced by accelerated carbonation in low and high calcium fly ash geopolymer concretes, Constr. Build. Mater., vol. 61, 2014, pp. 79–89.
[94] Fernandez-Jimenez, A. et al., Steel passive state stability in activated fly ash mortars, Mater. Construccion., vol. 60, No. 300, 2010, pp. 51–65.
[95] Miranda, J. et al., Corrosion resistance in activated fly ash mortars, Cem. Concr. Res., vol. 35, No. 6, 2005, pp. 1210–1217.
[96] Temuujin, J. et al., Preparation of metakaolin based geopolymer coatings on metal substrates as thermal barriers, Appl. Clay Sci., vol. 46, No. 3, 2009, pp. 265–270.
[97] Temuujin, J. et al., Fly ash based geopolymer thin coatings on metal substrates and its thermal evaluation, J. Hazard. Mater., vol. 180, No. 3, 2010, pp. 748–752.
[98] Temuujin, J. et al., Preparation and thermal properties of fire resistant metakaolin-based geopolymer-type coatings, J. Non-Cryst. Solids., vol. 357, No. 5, 2011, pp. 1399–1404.
[99] Latella, B. et al., Adhesion of glass to steel using a geopolymer, J. Mater. Sci., vol. 41, No. 4, 2006, pp. 1261–1264.
[100] De Barros, S. et al., Adhesion of Geopolymer Bonded Joints Considering Surface Treatments, J. Adhes., vol. 88, No. 4-6, 2012, pp. 364–375.
[101] Lichvar, P. et al., Behaviour of aluminosilicate inorganic matrix sial during and after solidification of radioactive sludge and radioactive spent resins and their mixtures, Amec Nuclear Slovakia, 2010.
[102] Mimura, H. et al., Adsorption behavior of cesium and strontium on synthetic zeolite-P, J. Nucl. Sci. Technol., vol. 30, No. 5, 1993, pp. 436–443.
[103] Xu, Z. et al., Immobilization of strontium-loaded zeolite A by metakaolin based-geopolymer, Ceram. Int., vol. 43, No. 5, 2017, pp. 4434–4439.
[104] Lahalle, H., Le conditionnement de l'aluminium métallique dans les ciments phosphomagnésiens, Université de Bourgogne, 2016, thesis (in French).
[105] Kuenzel, C. et al., Encapsulation of aluminium in geopolymers produced from metakaolin, J. Nucl. Mater., vol.447, No. 1-3, 2014, pp. 208–214.
[106] Rooses, A. et al., Encapsulation of Mg–Zr alloy in metakaolin-based geopolymer, Appl. Clay Sci., vol. 73, 2013, pp. 86–92.
[107] Rooses, A. et al., Galvanic corrosion of Mg-Zr fuel cladding and steel immobilized in Portland cement and geopolymer at early ages, J. Nucl. Mater., vol. 435, No. 1-3, 2013, pp. 137–140.
[108] Gulbrandsen, E. et al., The passive behavior of Mg in alkaline fluoride solutions - electrochemical and electron-microscopic investigations, Corros. Sci., vol. 34, No. 9, 1993, pp. 1423–1440.
[109] Lambertin D., Use of anticorrosion agents for conditionning magnesium metal, conditioning material thus obtained, WO 2011120960 A1, 2011.

[110] Lambertin, D. et al., Method for dissolving a metal and use for packaging said metal in a geopolymer, FR3033444 A1, 2016.
[111] Blackford, M.G. et al., Transmission Electron Microscopy and Nuclear Magnetic Resonance Studies of Geopolymers for Radioactive Waste Immobilization, J. Am. Ceram. Soc., vol. 90, No. 4, 2007, pp. 1193–1199.
[112] Khalil, M.Y. et al., Immobilization of intermediate-level wastes in geopolymers, J. Nucl. Mater., vol. 211, No. 2, 1994, pp. 141–148.
[113] El-Naggar, M.R., Applicability of alkali activated slag-seeded Egyptian Sinai kaolin for the immobilization of ^{60}Co radionuclide, J. Nucl. Mater., vol. 447, No. 1-3, 2014, pp. 15–21.
[114] Hespe, E., Leach testing of immobilized radioactive waste solid - proposal for a standard method, At. Energy Rev., vol. 9, No. 1, 1971, p.195.
[115] Cantarel, V. et al., Solidification/stabilisation of liquid oil waste in metakaolin-based geopolymer, J. Nucl. Mater., vol. 464, 2015, pp. 16–19.
[116] Li, Z. et al., Method for processing contaminated water, JP2015231610 A, 2015.
[117] Li, Z. et al., Development of Paper Sludge Ash-Based Geopolymer and Application to Treatment of Hazardous Water Contaminated with Radioisotopes, Materials., vol. 9, No. 8, 2016, p. 633.
[118] Jamieson, E.J., Method for management of contaminants in alkaline process liquors, WO2008017109 A1, 2008.
[119] Meguro, Y. et al., Solidification of radioactive wastes using Alkali-activated materials "geopolymer", J. RANDEC, vol. 54, 2016, pp. 48-55, (in Japanese).
[120] Nakayama, J., Method for manufacturing solidified product of radioactive waste, JP2014035202 A 2015.
[121] Froehlich, H. et al., Process for the preparation of a solid waste product for the ultimate storage of radioactive substances, DE3840794 A1, 1990.
[122] Yamada, K. et al., Immobilizing material for radioactive substance and processing method of radioactive contaminant, JP2013190257 A, 2013.
[123] Gong, W. et al., Low-temperature solidification of radioactive and hazardous wastes, US20060211908 A1, 2006.
[124] Hussin, K. et al., Design and mixture for anti-radiation pozzolon-polymeric cementitious material, US20160260510 A1, 2016.
[125] Lambertin, D. et al., Influence of gamma ray irradiation on metakaolin based sodium geopolymer, J. Nucl. Mater., vol. 443, No. 1-3, 2013, pp. 311–315.
[126] Deng, N. et al., Effects of gamma-ray irradiation on leaching of simulated Cs-133(+) radionuclides from geopolymer wasteforms, J. Nucl. Mater., vol. 459, 2015, pp. 270–275.
[127] Takeda, H. et al., Rapid fabrication of highly dense geopolymers using a warm press method and their ability to absorb neutron irradiation, Constr. Build. Mater., vol. 50, 2014, pp. 82–86.
[128] Hata, K. et al., Hydrogen Peroxide Production by Gamma Radiolysis of Sodium Chloride Solutions Containing a Small Amount of Bromide Ion, Nucl. Technol., vol. 193, No. 3, 2016, pp. 434–443.
[129] Hata, K. et al., Simulation for radiolytic products of seawater: effects of seawater constituents, dilution rate, and dose rate, J. Nucl. Sci. Technol., vol. 53, No. 8, 2016, pp. 1183–1191.
[130] Kumagai, Y. et al., Hydrogen production in gamma radiolysis of the mixture of mordenite and seawater, J. Nucl. Sci. Technol., vol. 50, No. 2, 2013, pp. 130–138.
[131] Yamagishi, I. et al., Characterization and storage of radioactive zeolite waste, J. Nucl. Sci. Technol., vol. 51, No. 7-8, 2014, pp. 1044–1053.
[132] Vance, E.R. et al., 18 - Geopolymers for nuclear waste immobilisation, in: Provis, J.L., van Deventer J.S.J., Geopolymers, Woodhead Publishing, 2009, pp. 401–420.

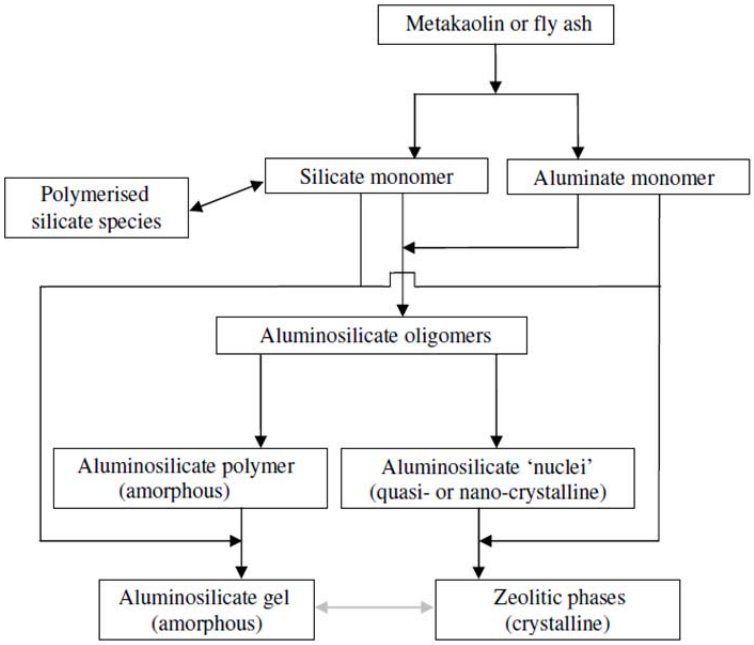

Figure 1 Schematic representation of Provis reaction model [2] between an activating alkaline solution and an aluminosilicate source with a low calcium content

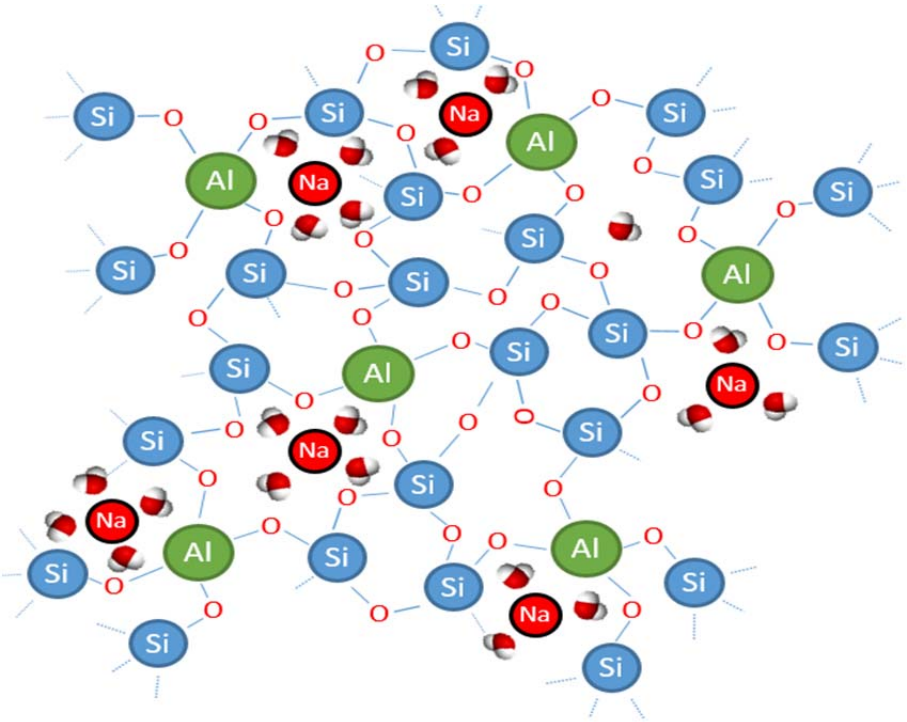

Figure 2 Representation of the structure of a sodium based geopolymer

Formulation parameter / Macroscopic property	Cation Na → K → Cs	M/Al molar ratio M= Na, K or Cs	Si/Al molar ratio	Water content	Aluminosilicate spec. surface and amorphous content
Setting time	∝ - (*)	~ - 強	ʘ - 弱	ʘ - 弱	~ - 強
Paste viscosity	~ - 弱		∝ - 弱	~ - 強	~ - 強
Pore size	~ - 強		~ - 弱	ʘ - 強	
Mechanical strengh	~ - (*)	∝ - 弱	ʘ - 強	~ - 強	

∝	Increase in the formulation parameter induces an increase of the macroscopic property.
~	Increase in the formulation parameter induces a decrease of the macroscopic property.
ʘ	An optimum for the formulation parameter can be found.
強	Strong impact of the formulation parameter on the macroscopic property
弱	Small impact of the formulation parameter on the macroscopic property
(*)	Cs geopolymer are uncomparable to Na and K geopolymers.
	Unknown, irrelevent or subject to discussion

Figure 3 Representation of the relations between macroscopic properties and formulation parameters

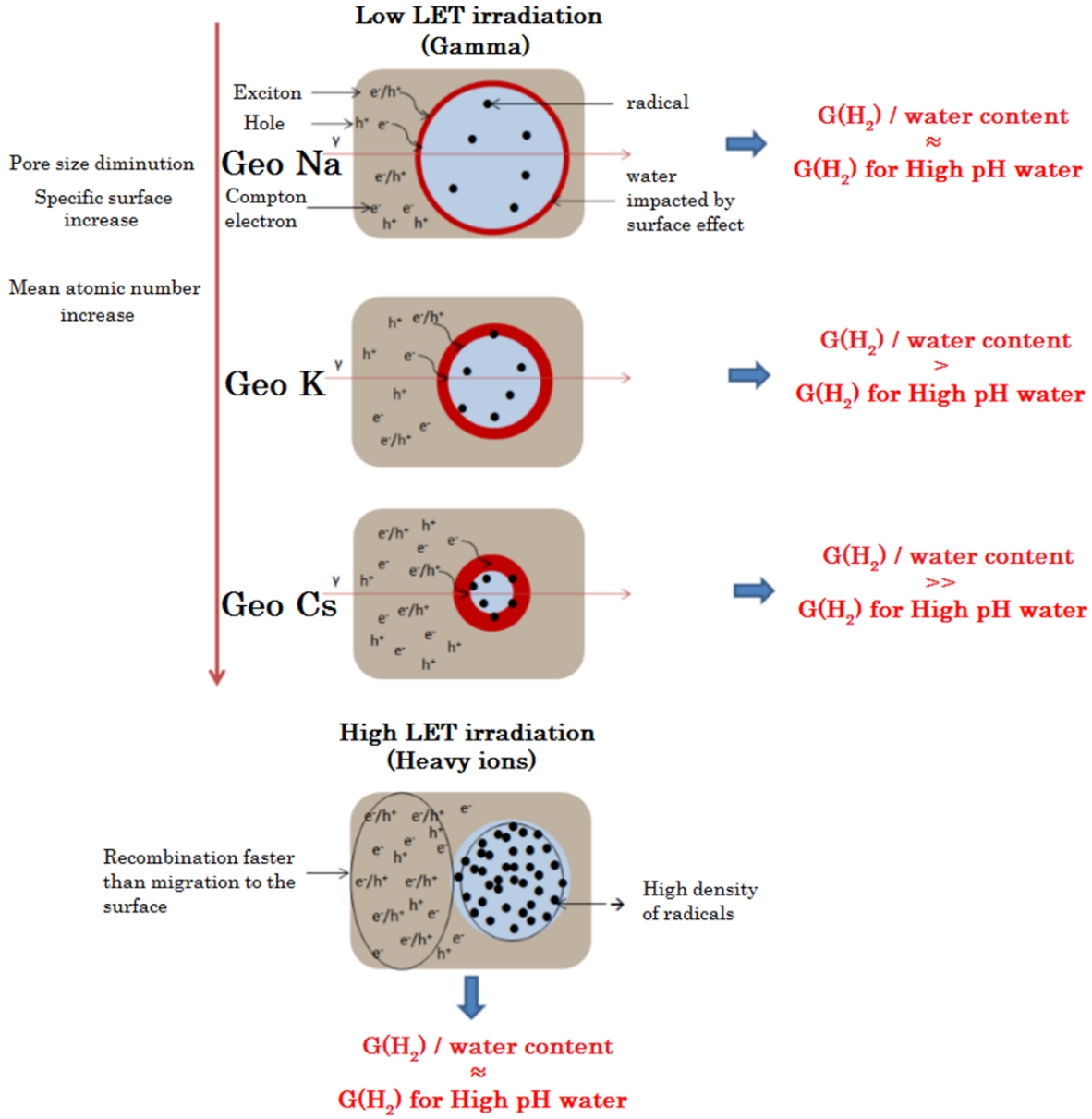

Figure 4 Schematic representation by F. Chupin [23] (translated) of water radiolysis in geopolymer under gamma or heavy ion irradiation

Table 1 Specific surface, mean pore diameter and pore volume obtained by P. Steins [48] with geopolymer having the same formulation: 1.8 Si/M ; 1 Al/M ; 11.5 H_2O/M with M = Na, K or Cs

	Specific surface (BET)	**Mean pore diameter (BJH)**	**Pore volume (BJH)**
Na-Geopolymer	54 m^2/g	102 Å	0.18 cm^3/g
K-Geopolymer	123 m^2/g	65 Å	0.28 cm^3/g
Cs-Geopolymer	237 m^2/g	36 Å	0.27 cm^3/g

Table 2 Studies and patents about geopolymer as a matrix for nuclear wastes ordered by country

Country	Subject / Waste	Reference
Australia	Cs & Sr salts	[8],[111]
China	Sr loaded zeolite	[103]
Egypt	Co	[113]
	NO_3 salts	[112]
France	Organic liquids	[26],[115]
	Mg-Zr alloys	[106],[107]
Germany	Graphite	AIEA Doc.
	NO_3 salts	[112]
	Undefined waste	[121]
Japan	Contaminated water	[116],[117]
	Undefined wastes	[120],[122]
	Fukushima secondary wastes	[119]
Malaysia	Undefined Waste	[124]
U.K.	Al metal	[105]
	Cs & Sr hydroxide	[54]
	Zeolite	[54]
U.S.A.	Undefined Wastes	[123]
Slovakia	Sludge & Resins	[101]

Table 3 Cs leaching results of Deng et al. [126]

Leaching medium	Condition	Diffusion coefficient	Leaching index
Deionized water	Non-irradiated	1.86×10^{-11}	10.7
	Irradiated	2.64×10^{-11}	10.6
Ground water	Non-irradiated	4.66×10^{-11}	10.3
	Irradiated	7.54×10^{-11}	10.1
Sea water	Non-irradiated	7.79×10^{-10}	9.2
	Irradiated	1.91×10^{-9}	8.7

国際単位系（SI）

表１．SI 基本単位

基本量	SI 基本単位	
	名称	記号
長さ	メートル	m
質量	キログラム	kg
時間	秒	s
電流	アンペア	A
熱力学温度	ケルビン	K
物質量	モル	mol
光度	カンデラ	cd

表２．基本単位を用いて表されるSI組立単位の例

組立量	SI 組立単位	
	名称	記号
面積	平方メートル	m^2
体積	立方メートル	m^3
速さ，速度	メートル毎秒	m/s
加速度	メートル毎秒毎秒	m/s^2
波数	毎メートル	m^{-1}
密度，質量密度	キログラム毎立方メートル	kg/m^3
面積密度	キログラム毎平方メートル	kg/m^2
比体積	立方メートル毎キログラム	m^3/kg
電流密度	アンペア毎平方メートル	A/m^2
磁界の強さ	アンペア毎メートル	A/m
量濃度(a)，濃度	モル毎立方メートル	mol/m^3
質量濃度	キログラム毎立方メートル	kg/m^3
輝度	カンデラ毎平方メートル	cd/m^2
屈折率(b)	（数字の） 1	1
比透磁率(b)	（数字の） 1	1

(a) 量濃度（amount concentration）は臨床化学の分野では物質濃度（substance concentration）ともよばれる。
(b) これらは無次元量あるいは次元１をもつ量であるが、そのことを表す単位記号である数字の１は通常は表記しない。

表３．固有の名称と記号で表されるSI組立単位

組立量	SI 組立単位			
	名称	記号	他のSI単位による表し方	SI基本単位による表し方
平面角	ラジアン(b)	rad	1 (b)	m/m
立体角	ステラジアン(b)	sr(c)	1 (b)	m^2/m^2
周波数	ヘルツ(d)	Hz		s^{-1}
力	ニュートン	N		$m\ kg\ s^{-2}$
圧力，応力	パスカル	Pa	N/m^2	$m^{-1}\ kg\ s^{-2}$
エネルギー，仕事，熱量	ジュール	J	N m	$m^2\ kg\ s^{-2}$
仕事率，工率，放射束	ワット	W	J/s	$m^2\ kg\ s^{-3}$
電荷，電気量	クーロン	C		s A
電位差（電圧），起電力	ボルト	V	W/A	$m^2\ kg\ s^{-3}\ A^{-1}$
静電容量	ファラド	F	C/V	$m^{-2}\ kg^{-1}\ s^4\ A^2$
電気抵抗	オーム	Ω	V/A	$m^2\ kg\ s^{-3}\ A^{-2}$
コンダクタンス	ジーメンス	S	A/V	$m^{-2}\ kg^{-1}\ s^3\ A^2$
磁束	ウエーバ	Wb	Vs	$m^2\ kg\ s^{-2}\ A^{-1}$
磁束密度	テスラ	T	Wb/m^2	$kg\ s^{-2}\ A^{-1}$
インダクタンス	ヘンリー	H	Wb/A	$m^2\ kg\ s^{-2}\ A^{-2}$
セルシウス温度	セルシウス度(e)	℃		K
光束	ルーメン	lm	cd sr(c)	cd
照度	ルクス	lx	lm/m^2	m^{-2} cd
放射性核種の放射能(f)	ベクレル(d)	Bq		s^{-1}
吸収線量，比エネルギー分与，カーマ	グレイ	Gy	J/kg	$m^2\ s^{-2}$
線量当量，周辺線量当量，方向性線量当量，個人線量当量	シーベルト(g)	Sv	J/kg	$m^2\ s^{-2}$
酸素活性	カタール	kat		s^{-1} mol

(a)SI接頭語は固有の名称と記号を持つ組立単位と組み合わせても使用できる。しかし接頭語を付した単位はもはやコヒーレントではない。
(b)ラジアンとステラジアンは数字の１に対する単位の特別な名称で、量についての情報をつたえるために使われる。実際には、使用する時には記号radおよびsrが用いられるが、習慣として組立単位としての記号である数字の１は明示されない。
(c)測光学ではステラジアンという名称と記号srを単位の表し方の中に、そのまま維持している。
(d)ヘルツは周期現象についてのみ、ベクレルは放射性核種の統計的過程についてのみ使用される。
(e)セルシウス度はケルビンの特別な名称で、セルシウス温度を表すために使用される。セルシウス度とケルビンの単位の大きさは同一である。したがって、温度差や温度間隔を表す数値はどちらの単位で表しても同じである。
(f)放射性核種の放射能（activity referred to a radionuclide）は、しばしば誤った用語で"radioactivity"と記される。
(g)単位シーベルト（PV,2002,70,205）についてはCIPM勧告2（CI-2002）を参照。

表４．単位の中に固有の名称と記号を含むSI組立単位の例

組立量	SI 組立単位		
	名称	記号	SI 基本単位による表し方
粘度	パスカル秒	Pa s	$m^{-1}\ kg\ s^{-1}$
力のモーメント	ニュートンメートル	N m	$m^2\ kg\ s^{-2}$
表面張力	ニュートン毎メートル	N/m	$kg\ s^{-2}$
角速度	ラジアン毎秒	rad/s	$m\ m^{-1}\ s^{-1}=s^{-1}$
角加速度	ラジアン毎秒毎秒	rad/s^2	$m\ m^{-1}\ s^{-2}=s^{-2}$
熱流密度，放射照度	ワット毎平方メートル	W/m^2	$kg\ s^{-3}$
熱容量，エントロピー	ジュール毎ケルビン	J/K	$m^2\ kg\ s^{-2}\ K^{-1}$
比熱容量，比エントロピー	ジュール毎キログラム毎ケルビン	J/(kg K)	$m^2\ s^{-2}\ K^{-1}$
比エネルギー	ジュール毎キログラム	J/kg	$m^2\ s^{-2}$
熱伝導率	ワット毎メートル毎ケルビン	W/(m K)	$m\ kg\ s^{-3}\ K^{-1}$
体積エネルギー	ジュール毎立方メートル	J/m^3	$m^{-1}\ kg\ s^{-2}$
電界の強さ	ボルト毎メートル	V/m	$m\ kg\ s^{-3}\ A^{-1}$
電荷密度	クーロン毎立方メートル	C/m^3	m^{-3} s A
表面電荷	クーロン毎平方メートル	C/m^2	m^{-2} s A
電束密度，電気変位	クーロン毎平方メートル	C/m^2	m^{-2} s A
誘電率	ファラド毎メートル	F/m	$m^{-3}\ kg^{-1}\ s^4\ A^2$
透磁率	ヘンリー毎メートル	H/m	$m\ kg\ s^{-2}\ A^{-2}$
モルエネルギー	ジュール毎モル	J/mol	$m^2\ kg\ s^{-2}\ mol^{-1}$
モルエントロピー，モル熱容量	ジュール毎モル毎ケルビン	J/(mol K)	$m^2\ kg\ s^{-2}\ K^{-1}\ mol^{-1}$
照射線量（X線及びγ線）	クーロン毎キログラム	C/kg	kg^{-1} s A
吸収線量率	グレイ毎秒	Gy/s	$m^2\ s^{-3}$
放射強度	ワット毎ステラジアン	W/sr	$m^4\ m^{-2}\ kg\ s^{-3}=m^2\ kg\ s^{-3}$
放射輝度	ワット毎平方メートル毎ステラジアン	$W/(m^2\ sr)$	$m^2\ m^{-2}\ kg\ s^{-3}=kg\ s^{-3}$
酵素活性濃度	カタール毎立方メートル	kat/m^3	$m^{-3}\ s^{-1}$ mol

表５．SI 接頭語

乗数	名称	記号	乗数	名称	記号
10^{24}	ヨタ	Y	10^{-1}	デシ	d
10^{21}	ゼタ	Z	10^{-2}	センチ	c
10^{18}	エクサ	E	10^{-3}	ミリ	m
10^{15}	ペタ	P	10^{-6}	マイクロ	μ
10^{12}	テラ	T	10^{-9}	ナノ	n
10^9	ギガ	G	10^{-12}	ピコ	p
10^6	メガ	M	10^{-15}	フェムト	f
10^3	キロ	k	10^{-18}	アト	a
10^2	ヘクト	h	10^{-21}	ゼプト	z
10^1	デカ	da	10^{-24}	ヨクト	y

表６．SIに属さないが、SIと併用される単位

名称	記号	SI 単位による値
分	min	1 min=60 s
時	h	1 h =60 min=3600 s
日	d	1 d=24 h=86 400 s
度	°	1°=(π/180) rad
分	’	1’=(1/60)°=(π/10 800) rad
秒	”	1”=(1/60)’=(π/648 000) rad
ヘクタール	ha	1 ha=1 $hm^2=10^4m^2$
リットル	L, l	1 L=1 l=1 $dm^3=10^3cm^3=10^{-3}m^3$
トン	t	1 t=10^3 kg

表７．SIに属さないが、SIと併用される単位で、SI単位で表される数値が実験的に得られるもの

名称	記号	SI 単位で表される数値
電子ボルト	eV	1 eV=1.602 176 53(14)×10^{-19}J
ダルトン	Da	1 Da=1.660 538 86(28)×10^{-27}kg
統一原子質量単位	u	1 u=1 Da
天文単位	ua	1 ua=1.495 978 706 91(6)×10^{11}m

表８．SIに属さないが、SIと併用されるその他の単位

名称	記号	SI 単位で表される数値
バール	bar	1 bar=0.1MPa=100 kPa=10^5Pa
水銀柱ミリメートル	mmHg	1 mmHg≈133.322Pa
オングストローム	Å	1 Å=0.1nm=100pm=10^{-10}m
海里	M	1 M=1852m
バーン	b	1 b=100fm^2=$(10^{-12}cm)^2$=$10^{-28}m^2$
ノット	kn	1 kn=(1852/3600)m/s
ネーパ	Np	SI単位との数値的な関係は、対数量の定義に依存。
ベル	B	
デシベル	dB	

表９．固有の名称をもつCGS組立単位

名称	記号	SI 単位で表される数値
エルグ	erg	1 erg=10^{-7} J
ダイン	dyn	1 dyn=10^{-5}N
ポアズ	P	1 P=1 dyn s cm^{-2}=0.1Pa s
ストークス	St	1 St =1$cm^2\ s^{-1}$=$10^{-4}m^2\ s^{-1}$
スチルブ	sb	1 sb =1cd cm^{-2}=10^4cd m^{-2}
フォト	ph	1 ph=1cd sr cm^{-2} =10^4lx
ガル	Gal	1 Gal =1cm s^{-2}=$10^{-2}ms^{-2}$
マクスウエル	Mx	1 Mx = 1G cm^2=10^{-8}Wb
ガウス	G	1 G =1Mx cm^{-2} =10^{-4}T
エルステッド(a)	Oe	1 Oe ≙ $(10^3/4\pi)$A m^{-1}

(a) ３元系のCGS単位系とSIでは直接比較できないため、等号「 ≙ 」は対応関係を示すものである。

表10．SIに属さないその他の単位の例

名称	記号	SI 単位で表される数値
キュリー	Ci	1 Ci=3.7×10^{10}Bq
レントゲン	R	1 R = 2.58×10^{-4}C/kg
ラド	rad	1 rad=1cGy=10^{-2}Gy
レム	rem	1 rem=1 cSv=10^{-2}Sv
ガンマ	γ	1 γ=1 nT=10^{-9}T
フェルミ		1 フェルミ=1 fm=10^{-15}m
メートル系カラット		1 メートル系カラット= 0.2 g = 2×10^{-4}kg
トル	Torr	1 Torr = (101 325/760) Pa
標準大気圧	atm	1 atm = 101 325 Pa
カロリー	cal	1 cal=4.1858J（「15℃」カロリー），4.1868J（「IT」カロリー），4.184J（「熱化学」カロリー）
ミクロン	μ	1 μ =1μm=10^{-6}m

（第8版，2006年）